

Faculdade de Engenharia da Universidade do Porto



Broadband Feed for a Parabolic Antenna for Satellite Tracking

Frederico José Teixeira Moreira

Final Version

MSc Thesis developed in the scope of the
Integrated Master in Electrical and Computers Engineering
Telecommunications Major

Supervisor: Sérgio Reis Cunha (PhD)

January 2011

Resumo

Actualmente, o processo de telecomunicações no mundo inteiro requer transmissões rápidas e baratas. Obedecendo a isso, as antenas de banda larga são parte da solução para estabelecer um conceito de utilização de extensas larguras de banda às altas frequências. Deste modo, os sistemas de satélite têm muitas potencialidades para tornar o mundo numa pequena aldeia global. Como exemplo, os satélites de hoje servem a humanidade em áreas tão extensas como a navegação ou a meteorologia.

Tendo em conta o referido, a pesquisa efectuada nesta tese é centrada na implementação de uma antena espiral equiangular e planar, capaz de alimentar uma antena parabólica de forma coerente. De facto, ela reúne várias características que são importantes para alimentar correctamente uma antena parabólica, a fim de permitir uma comunicação estável com os satélites que se pretende monitorizar. Tal antena é também conhecida como uma antena de banda larga, que é caracterizada por parâmetros vitais como a relação de ondas estacionárias (VSWR), impedância de entrada, padrão de radiação, coeficiente de reflexão, entre outros.

Por fim, as medições dos parâmetros da antena espiral equiangular e planar, foram feitas com a ajuda de programas de simulação (*Ansoft HFSS*), sendo posteriormente comparadas com resultados experimentais obtidos no analisador de rede vectorial e na câmara anecóica.

Abstract

Currently, world telecommunications require fast and cheap transmissions. Concerning to that, broadband antennas are part of the solution to establish a concept of wideband frequency usage. Thus, satellite systems have many potentialities to make the world a small global village. As an example, satellites of nowadays can serve humankind in such areas as navigation or weather forecast.

Concerning to that, the research of this thesis is focused on the implementation of a planar equiangular spiral antenna, which can gather several characteristics that are important to feed properly a parabolic antenna, in order to enable a good communication with satellites that can be tracked. Such antenna is a broadband antenna that is characterised by vital parameters as voltage standing wave ratio, input impedance, radiation pattern, reflection coefficient, between others.

Finally, the measurements of those antenna parameters were made using software simulation (*Ansoft HFSS*) and were compared to experimental results obtained from an anechoic chamber and from a vector network analyser.

Acknowledgements

I am pleased to acknowledge the advice and ideas of Professor Sérgio Reis Cunha, to whom must be endorsed all the credit for the imaginative notions leading to the design of equiangular spiral antenna. It was a pleasure to work with such a dedicated person.

I want to thank my friends Mário Pereira and Qi Luo for the help they provided me.

I must also acknowledge André Vidal and André Paiva, without whose motivation and encouragement I would not finish my thesis on time.

I would like to express my sincere gratitude to all my friends and family, especially to Eduardo Magalhães for all the support during my entire thesis, and to my best friend Tó Zé who was always encouraging me all the time.

And finally, infinite thanks to my purple cat who was always with me.

"Happiness is always there; where you look for it."

Unknown Author

Index

Resumo.....	i
Abstract.....	iii
Acknowledgements.....	v
Index.....	ix
List of Figures.....	xiii
List of Tables.....	xvii
Symbols and Acronyms.....	xix
Chapter 1.....	1
Introduction.....	1
1.1 Motivation.....	1
1.2 Objectives.....	2
1.3 Methodology.....	2
1.4 Structure of the Thesis.....	3
Chapter 2.....	5
Literature Review.....	5
2.1 Introduction to antennas.....	5
2.2 Radio-Frequency.....	7
2.3 Antenna Parameters.....	9
2.3.1 Radiation Pattern.....	9
2.3.2 Half-Power Beamwidth.....	11
2.3.3 Directivity.....	12
2.3.4 Gain.....	12
2.3.5 Efficiency.....	14
2.3.6 Scattering Parameters.....	15
2.3.7 Voltage Standing Wave Ratio.....	17
2.3.8 Polarisation.....	19
2.3.9 Input Impedance.....	20
2.3.10 Bandwidth.....	21
2.3.11 Reciprocity.....	23
2.4 Types of Antennas.....	23
2.4.1 Wire Antennas.....	23
2.4.2 Aperture Antennas.....	25

2.4.3 Microstrip Antennas	25
2.4.4 Reflector Antennas	25
2.4.5 Travelling Wave Antennas	26
2.5 Broadband Antennas	26
2.6 Frequency Independent Antennas	27
2.6.1 Introduction	27
2.6.2 Analytical Description	27
2.7 Planar Equiangular Spiral Antenna	29
2.7.1 Planar Equiangular Spiral Antenna Feeding	31
2.8 Satellite Systems	31
2.8.1 Satellite Orbits.....	33
Chapter 3	37
Work Description	37
3.1 The Choice of Planar Equiangular Spiral Antenna	37
3.2 The implementation of the feed	37
3.2.1 Design.....	38
3.2.2 Fabrication	42
Chapter 4	47
Software Simulation.....	47
4.1 Return Loss	47
4.2 Voltage Standing Wave Ratio	49
4.3 Radiation Pattern	51
4.3.1 Simulation of f2.....	52
4.3.2 Simulation of f1	54
4.3.3 Simulation of f3.....	55
4.3.4 Simulation of f4.....	56
4.3.5 Simulation of f5.....	57
Chapter 5	59
Experimental Results	59
5.1 Return Loss and Voltage Standing Wave Ratio Measurements	59
5.1.1 Return Loss.....	60
5.1.2 Voltage Standing Wave Ratio	61
5.2 Radiation Pattern measurements.....	62
5.2.1 Measurement of f1	64
5.2.2 Measurement of f2	65
5.2.3 Measurement of f3	67
5.2.4 Measurement of f4	68
5.2.5 Measurement of f5	70
Chapter 6	73
Conclusions and Future Work	73
6.1 Analysis and review	73
6.2 Future Work	74
References.....	77
Appendix A.....	79
Matlab Code	79
Appendix B.....	81

Calibration Types	81
-------------------------	----

List of Figures

Figure 2.1 - The antenna as a transition structure, for a transmitting antenna and for a receiving antenna [3]	5
Figure 2.2 - Circuit representing antenna as whole structure [1]	7
Figure 2.3 - Wavelength measurement	8
Figure 2.4 - Frequency quality	8
Figure 2.5 - Electromagnetic spectrum [4]	8
Figure 2.6 - Spherical coordinate system which describes the radiation pattern (adapted from [4])	10
Figure 2.7 - Polar diagram of the azimuth plane radiation pattern [5]	10
Figure 2.8 - Three-dimensional directional radiation pattern [5]	10
Figure 2.9 - Polar diagram of the elevation plane radiation pattern [5]	10
Figure 2.10 - Polar diagram of the azimuth plane radiation pattern [5]	10
Figure 2.11 - Three-dimensional omnidirectional radiation pattern [5]	10
Figure 2.12 - Polar diagram of the elevation plane radiation pattern [5]	10
Figure 2.13 - Radiation pattern lobes	11
Figure 2.14 - Rectangular diagram of HPBW (adapted from [5])	12
Figure 2.15 - Polar diagram of HPBW (adapted from [5])	12
Figure 2.16 - Two-port network constituted by S-parameters	15
Figure 2.17 - Helical antenna with RHCP [8]	19
Figure 2.18 - An airplane antenna emitting [9]	19
Figure 2.19 - Circuit representing input impedance at the entrance terminals of the transmission line.....	21
Figure 2.20 - Frequency bandwidth for VSWR parameter	22

Figure 2.21 - The wavelength of a dipole antenna [14]	24
Figure 2.22 - Translation and rotation processes to scale a frequency independent antenna [17]	29
Figure 2.23 - Planar Equiangular Spiral antenna curve [13]	30
Figure 2.24 - Bi-directional communication between ground segments through a satellite station	32
Figure 2.25 - Orbital altitudes of satellites (adapted from [20])	34
Figure 2.26 - Coordinate system describing a ground station-satellite communication	35
Figure 3.1 - PESA plot in <i>MATLAB</i>	38
Figure 3.2 - The intersection points in order to create finite arms	39
Figure 3.3 - The desired final shape of PESA	39
Figure 3.4 - PESA model in <i>Ansoft HFSS</i> as a whole: front and back sides of the designed PCB.....	40
Figure 3.5 - A close-up of lumped port (red color) at the origin.....	40
Figure 3.6 - A close-up of BNC RF connector	41
Figure 3.7 - The PCB inside an air box - with a reflector on the right	41
Figure 3.8 - The PCB of PESA - left part represents the top and right part represents the bottom.....	43
Figure 3.9 - The PCB of PESA fed by a coaxial cable RG-174/U connected to a BNC RF connector	43
Figure 3.10 - Feeding of PESA structure in detail.....	44
Figure 3.11 - Metallic reflector	45
Figure 4.1 - Simulated return loss for PESA without reflector	47
Figure 4.2 - Simulated return loss for PESA with reflector	48
Figure 4.3 - PESA return loss with reflector vs. PESA return loss without reflector.....	49
Figure 4.4 - Simulated VSWR for PESA without reflector	50
Figure 4.5 - Simulated VSWR for PESA with reflector	50
Figure 4.6 - PESA VSWR with reflector vs. PESA VSWR without reflector.....	51
Figure 4.7 - Three-dimensional plot of simulated radiation pattern for $f_2 = 1.5$ GHz (PESA without reflector).....	52
Figure 4.8 - Polar plot of simulated radiation pattern for $f_2 = 1.5$ GHz (PESA without reflector).....	52

Figure 4.9 - Three-dimensional plot of simulated radiation pattern for $f_2 = 1.5$ GHz (PESA with reflector)	53
Figure 4.10 - Polar plot of simulated radiation pattern for $f_2 = 1.5$ GHz (PESA with reflector)	53
Figure 4.11 - Three-dimensional plot of simulated radiation pattern for $f_1 = 1.274$ GHz	54
Figure 4.12 - Polar plot of simulated radiation pattern for $f_1 = 1.274$ GHz	55
Figure 4.13 - Three-dimensional plot of simulated radiation pattern for $f_3 = 1.69$ GHz	55
Figure 4.14 - Polar plot of simulated radiation pattern for $f_3 = 1.274$ GHz	56
Figure 4.15 - Three-dimensional plot of simulated radiation pattern for $f_4 = 2.384$ GHz	56
Figure 4.16 - Polar plot of simulated radiation pattern for $f_4 = 2.384$ GHz	56
Figure 4.17 - Three-dimensional plot of simulated radiation pattern for $f_5 = 2.516$ GHz	57
Figure 4.18 - Polar plot of simulated radiation pattern for $f_4 = 2.516$ GHz	58
Figure 5.1 - Vector Network Analyser (VNA)	60
Figure 5.2 - Return loss measurement	60
Figure 5.3 - VSWR measured.....	61
Figure 5.4 - Measurement of PESA (antenna under test) at the anechoic chamber.....	63
Figure 5.5 - A log-periodic antenna acting as a trasnmitter (source antenna) at the anechoic chamber	63
Figure 5.6 - Polar plot of the radiation pattern of E_ϕ measured for $f_1 = 1.274$ GHz	64
Figure 5.7 - Polar plot of the radiation pattern of E_θ measured for $f_1 = 1.274$ GHz.....	64
Figure 5.8 - Comparison between polar plots of E_ϕ and E_θ radiation patterns measured for $f_1 = 1.274$ GHz.....	65
Figure 5.9 - Polar plot of the radiation pattern of E_ϕ measured for $f_2 = 1.58$ GHz.....	65
Figure 5.10 - Polar plot of the radiation pattern of E_θ measured for $f_2 = 1.58$ GHz.....	66
Figure 5.11 - Comparison between polar plots of E_ϕ and E_θ radiation patterns measured for $f_2 = 1.58$ GHz	66
Figure 5.12 - Polar plot of the radiation pattern of E_ϕ measured for $f_3 = 1.69$ GHz.....	67
Figure 5.13 - Polar plot of the radiation pattern of E_θ measured for $f_3 = 1.69$ GHz.....	67
Figure 5.14 - Comparison between polar plots of E_ϕ and E_θ radiation patterns measured for $f_3 = 1.69$ GHz	68
Figure 5.15 - Polar plot of the radiation pattern of E_ϕ measured for $f_4 = 2.384$ GHz	68
Figure 5.16 - Polar plot of the radiation pattern of E_θ measured for $f_4 = 2.384$ GHz	69

Figure 5.17 - Comparison between polar plots of E_φ and E_θ radiation patterns measured for $f_4 = 2.348$ GHz	69
Figure 5.18 - Polar plot of the radiation pattern of E_φ measured for $f_5 = 2.516$ GHz	70
Figure 5.19 - Polar plot of the radiation pattern of E_θ measured for $f_5 = 2.516$ GHz	70
Figure 5.20 - Comparison between polar plots of E_φ and E_θ radiation patterns measured for $f_5 = 2.516$ GHz	71
Figure 6.1 - Parabolic antenna which will be part of a future work	75

List of Tables

Table 2.1 - Radio spectrum bands (www.vlf.it/frequency/bands.html)	9
Table 2.2 - VSWR in numbers	18
Table 2.3 - Different orbit properties [20]	34
Table 4.1 - Markers values for figure Figure 4.1	48
Table 4.2 - Marker values for Figure 4.2	49
Table 4.3 - Marker values for Figure 4.4	50
Table 4.4 - Marker values for Figure 4.5	51
Table 4.5 - Gain comparison of different PESA configuration for $f_2 = 1.5$ GHz	54
Table 4.4 - HPBW comparison of different PESA configurations for $f_2 = 1.5$ GHz	54
Table 5.1 - Return loss along several frequencies drawn in Figure 5.2	61
Table 5.2 - VSWR along several frequencies drawn in Figure 5.3	62
Table 5.3 - HPBW for the several tested frequencies	71
Table 6.1 - Measured values for radiation pattern measurements	74
Table 6.2 - Simulated values for radiation pattern simulations	74

Symbols and Acronyms

List of acronyms

AUT	<i>Antenna Under Test</i>
DEEC	Departamento de Engenharia Electrotécnica e Computadores
EM	<i>Electromagnetic</i>
FEUP	Faculdade de Engenharia da Universidade do Porto
GEO	<i>Geosynchronous Earth Orbit</i>
GSO	<i>Geostationary Earth Orbit</i>
HEO	<i>Highly Elliptical Orbit</i>
HF	<i>High Frequency</i>
HPBW	<i>Half-power Beamwidth</i>
LEO	<i>Low Earth Orbit</i>
LHCP	<i>Left-hand Circular Polarisation</i>
IL	<i>Insertion Loss</i>
ITU	<i>International Telecommunications Union</i>
MEO	<i>Medium Earth Orbit</i>
NGSO	<i>Non-geostationary Earth Orbit</i>
PCB	<i>Printed Circuit Board</i>
PESA	<i>Planar Equiangular Spiral Antenna</i>
TEM	<i>Transverse Electromagnetic Wave</i>
RHCP	<i>Right-hand Circular Polarisation</i>
RL	<i>Return Loss</i>
RF	<i>Radio-Frequency</i>
SATCOM	<i>Satellite Communication</i>
VNA	<i>Vector Network Analyser</i>
VSWR	<i>Voltage Standing Wave Ratio</i>

List of symbols

α	<i>Elevation</i>
β	<i>Azimuth</i>
Γ	<i>Reflection coefficient</i>

θ	<i>Elevation Plane</i>
λ	<i>Wavelength</i>
ρ	<i>Radial distance</i>
ρ_0	<i>Initial inner radius</i>
φ	<i>Azimuth Plane</i>
\emptyset	<i>Rotation angle with respect to x axis</i>
Ω	<i>Ohm</i>

Chapter 1

Introduction

In this introductory chapter the main reasons and motivation which contributed for the elaboration of the main subject of this thesis are presented: the creation of a suitable broadband feed possible to install in a parabolic antenna for tracking of satellites, located at the Faculty of Engineering of Porto University. Briefly, the objectives of the work are demoted, as well as its background methodology. Finally, it is exposed how this thesis is structured in order to give a better perspective to the reader.

1.1 Motivation

Nowadays, satellites communications play an important role in telecommunications. Two major elements of satellite communications systems are the space segment, where the satellite itself is orbiting and where the satellite control centre for station keeping of the satellite is, and the ground segment, which transmits the signal to the satellite and receives the signal from the satellite. Here one can find earth stations with rearward communication links and user terminals and interfaces, and also Network control centres. Antennas are the main part of this process, and they have the responsibility to receive, decode and convert the physical signal (the electromagnetic waves) into electric current, or vice-versa. The bandwidth of an antenna is specified in two ways, one definition is normally used for narrow band antennas and one is used for wide band antennas. Dealing with space communications require a parabolic antenna able to communicate with satellites operating at certain frequency ranges. Sometimes, some of those frequencies are unable to be reach and a more complex system is needed. Broadband antenna feeds are part of the solution. The term broadband is used for antennas that operate over a wide range of frequencies. A better definition of the term broadband could be: If the impedance and the radiation pattern of an antenna do not change significantly over about an octave ($f_{upper} / f_{lower} = 2$) or more, we will classify it as a broadband antenna. Many measurements require the acquisition of amplitude/phase data over wide or multiple frequency ranges and differing polarisations. The volume of data required to fully evaluate a test article is sufficiently large that high levels of measurement system automation are required to minimize test times and maximize test

facility usage. Therefore, broadband or multi-band compact range feeds with electronic polarisation selection are required for these applications.

1.2 Objectives

The main points of this thesis are to design, implement, calibrate, and test one or more broadband feeds of a parabolic antenna for tracking of satellites of Faculdade de Engenharia da Universidade do Porto (FEUP), located on the top of the building I-East, at the Departamento de Engenharia Electrotécnica e de Computadores (DEEC). Thus, it is wished to replace the existing feed (sensor element of the antenna) of narrowband by one or more feeds to be drawn, allowing the antenna to operate with satellites across all the useful spectrum of frequency, including VORSat. The latter is a very recent project created by FEUP that is still being developed. It mainly consists of a CubeSat with the purpose of measuring the satellite attitude from ground based on a set of RF signals transmitted from orbit, more specifically, a Low Earth Orbit (LEO).

Indeed, the parabolic antenna visible on the top of the building I-East is a 3-metre parabolic dish which has two degrees of freedom; so the tracking of any satellites is allowed. Its construction allows the receiving of signals of approximately 800 MHz up to a little bit more than 3 GHz; frequencies which are taken as a reference to build the antenna. Concerning to that, the GPS (Global Positioning System) frequencies L1 and L2, respectively of 1575.42 MHz and of 1227.6 MHz, are also planned frequencies to be tracked.

1.3 Methodology

This thesis is based on a strong component of practical measurements. The following procurement is explains the different steps of the developed work:

- Take note and make the comparative analysis of a set of possible designs of broadband feeds for the required parabolic antenna.
- Analyse how dense is the installation of the parabolic antenna and the detailed requirements of the job.
- Draw a feed or set of feeds for the antenna, studying with detail the same theory and using computer simulation.
- Implement the feed(s) using the manufactory process.
- Characterise and calibrate the feeds using a Vector Network Analyser (VNA).
- Install the feed(s), calibrate and test the antenna, obtaining calibration curves of the whole antenna plus feed.

1.4 Structure of the Thesis

This thesis is divided in six chapters.

This chapter is organised in four points: Motivation, objectives, methodology and structure of the thesis.

In chapter two, it is made the literature review, which is mainly about the most relevant subjects within antenna's field and satellite systems. It is given special attention to planar equiangular spiral antennas.

In chapter three, it is made a description of the work, explaining why the choice of the planar equiangular spiral antenna for this thesis. It is also described the implementation of the feed.

In chapter four, the software simulation of the designed antenna is focused.

Chapter five confers the experimental results obtained; it is made a detailed presentation of those respective measurements, followed by its explanation.

At last, chapter six is dedicated to the main conclusions of the obtained results, as well as the future work.

Chapter 2

Literature Review

In this chapter an approach to the topic of this thesis is made in order to contextualise the reader for what has been done so far in the field. One will start to read a brief presentation concerning to the theory of antennas, allowing the comprehension of its main features and parameters. Subsequently, it is given the necessary attention to the specific technology that supports this thesis work - the broadband feeds - also related to the referred frequency independent antennas. Finally, a study of the satellite systems and its associated communications with Earth antennas is presented.

2.1 Introduction to antennas

An antenna can be defined as a metallic device which radiates and receives electromagnetic waves (EM waves - see section 2.2), more specifically, radio waves [1]. Another possible explanation says that an antenna is the transition between a guided EM wave and a free-space EM wave [2], and vice-versa. This process is exemplified by a general communication between a transmitting antenna and a receiving antenna, as described in Figure 2.1.

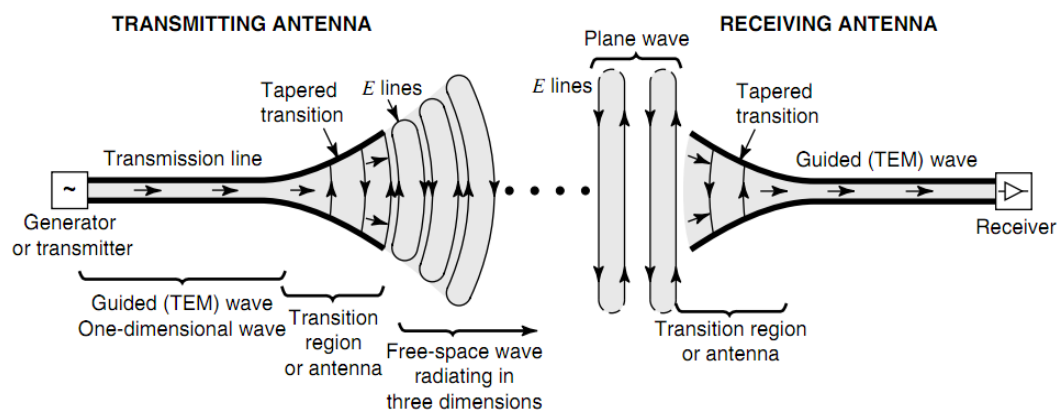


Figure 2.1 - The antenna as a transition structure, for a transmitting antenna and for a receiving antenna [3]

As shown above, for both antennas, the transmission line has the form of a coaxial line or a waveguide. The latter, when a transmitting antenna is considered, is connected to a transmitter that generates radio-frequency (RF - see section 2.2) energy that is guided through the uniform part of the line as a plane TEM wave with little loss, transformed into a signal that is amplified, modulated and applied to the antenna; otherwise, when a receiving antenna is considered, the transmission line is connected to a receiver which collects the alternating currents that resulted from the transformation process of the received radio waves by the antenna. Thus, we can also state that antennas convert electrons to photons¹ [3].

Antenna characteristics concerning to radiation are basically the same regardless of its type. Therefore, if a time-changing current or an acceleration (or deceleration) of charge occurs, the radiation will be created in a certain length of current element. This can be described by [1]:

$$L \cdot \frac{dI}{dt} = L \cdot q \cdot \frac{dv}{dt} \quad (\text{A.m/s}) \quad (2.1)$$

Where:

L - Length of the current element in metres (m);

$\frac{dI}{dt}$ - Time-changing current in ampere per second (A/s);

q - Elementary charge in coulomb (C) or (A.s). Note that $q = I \cdot t = 1.602 \times 10^{-19}$.

Furthermore, the radiation is always perpendicular to the acceleration and its power is proportional to the square of both parts of the equation (2.1). It is important to refer that the spacing between the two wires of the transition line is just a small part of a wavelength (see section 2.2); therefore, the more the transition curve of the antenna opens out the more the order of a wavelength or more is reached; consequently, the more the wave tends to be radiated and launched into the free-space [3].

Looking at the antenna structure as a whole, the transition region of the antenna is like a radiation resistance (R_r) to the transmission line point of view, which represents the radiation that the antenna emits, analysing it as a circuit. Figure 2 shows the complete circuit of an antenna; where the source is an ideal generator with a tension V_g (or V_s) and with an impedance Z_g (or Z_s); the transmission line is a line with characteristic impedance Z_c (or Z_0), and the antenna itself is represented by a load impedance Z_A that works as an input impedance which process will be explained in section 2.3.9 [1].

Therefore, if ideal conditions are applied, which are $Z_g = Z_c = Z_A$, the radiation resistance will get all the energy that is generated by the transmitter.

¹ A photon is an elementary particle composed by electromagnetic energy, and is the basic unit of light and all other forms of electromagnetic radiation. Its energy E is equal to $h \times f$, where h is the constant of Planck ($=6,63 \times 10^{-34}$ J s) and f is the frequency in Hz [3].

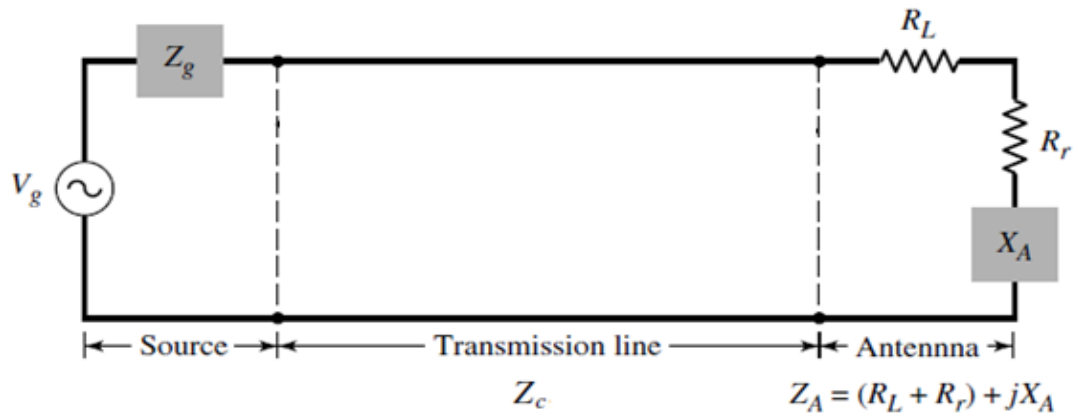


Figure 2.2 - Circuit representing antenna as whole structure [1]

2.2 Radio-Frequency

EM waves are a type of electromagnetic radiation which is organised according to the frequency (f) of its waves. Frequency counts the number of incidences that a repetition of an event occurs per unit of time. Usually, a frequency is given in Hertz (Hz) which means the number of cycles per second. Each cycle is also mentioned as a period (T). Therefore, frequency is the reciprocal of period:

$$f = \frac{1}{T} \quad (2.2)$$

Another very important parameter is the wavelength (λ), which is the distance between two consecutive points of the same phase, given in metres. Figure 2.3 shows the plot of wavelength and Figure 2.4 the difference between highest and lowest frequencies. The ratio of wavelength to frequency is given by:

$$f = \frac{c}{\lambda} \quad (2.3)$$

Where:

c - Speed of sound in free space, in metres per second (3×10^8 m/s).

The electromagnetic spectrum (Figure 2.5) is the diagram that covers a wide range of frequencies of electromagnetic radiation, such as: radio, microwave, infrared, visible light, ultraviolet, x-ray, and gamma ray. Radio waves have the lowest frequency and the highest wavelength, while for gamma rays is the opposite.

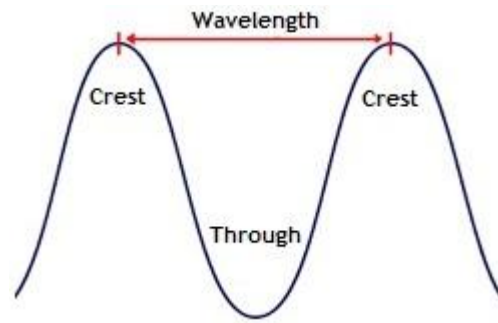


Figure 2.3 - Wavelength measurement

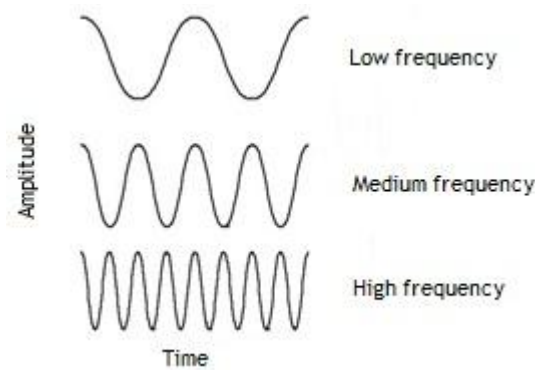


Figure 2.4 - Frequency quality

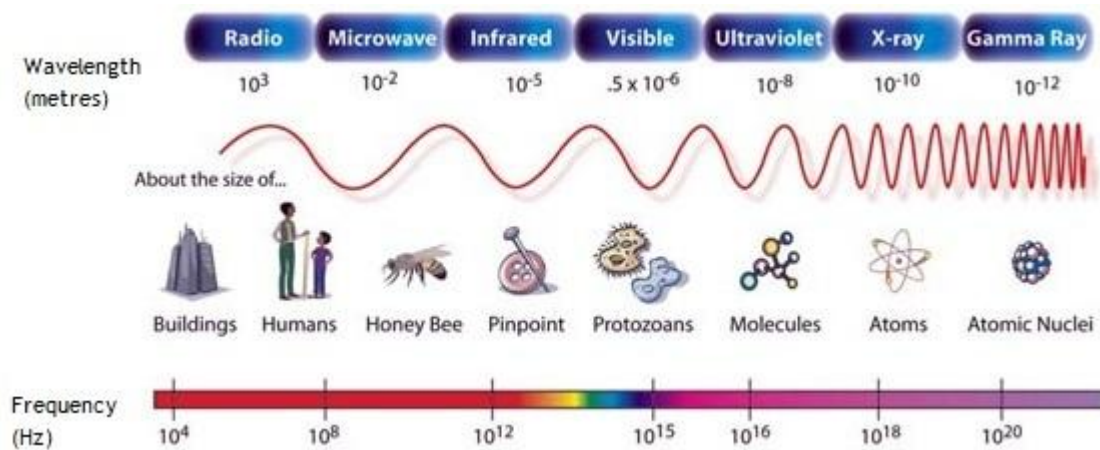


Figure 2.5 - Electromagnetic spectrum [4]

As seen above, the electromagnetic spectrum is divided into different frequency ranges. For the purpose of this thesis, the radio spectrum is the one used; therefore it will be focused. For telecommunications, International Telecommunications Union (ITU) is the entity which regulates the frequency spectrum usage, and determined that the usable spectrum is from 3 Hz to 300 GHz. Meanwhile, radio-frequency (RF) varies in a range of 30 kHz to 300 GHz, values for which radio waves start to be emitted in practice.

Table 2.1 describes the radio spectrum ranges for frequency and wavelength. [5]

Table 2.1 - Radio spectrum bands [5]

Radio spectrum	Frequency	Wavelength
Extremely low frequency (ELF)	3 Hz to 30 Hz	10000 km to 100000 km
Superlow frequency (SLF)	30 Hz to 300 Hz	1000 km to 10000 km
Ultralow frequency (ULF)	300 Hz to 3000 Hz	100 km to 1000 km
Very low frequency (VLF)	3 kHz to 30 kHz	10 km to 100 km
Low frequency (LF)	30 kHz to 300 kHz	1 km to 10 km
Medium frequency (MF)	300 kHz to 3000 kHz	100 m to 1 km
High frequency (HF)	3 MHz to 30 MHz	10 m to 100 m
Very high frequency (VHF)	30 MHz to 300 MHz	1 m to 10 m
Ultrahigh frequency (UHF)	300 MHz to 3000 MHz	10 cm to 1 m
Superhigh frequency (SHF)	3 GHz to 30 GHz	1 cm to 10 cm
Extremely high frequency (EHF)	30 GHz to 300 GHz	1 mm to 1 cm

2.3 Antenna Parameters

Antennas are defined by several parameters according to their constitution and shape. In this section, the most important are considered and explained, and an overview of each is essential to describe antenna's performance.

2.3.1 Radiation Pattern

The radiation pattern is a graphical (three-dimensional or two-dimensional) or a mathematical illustration of the radiation properties of an antenna as a function of the space coordinates defined by the spherical coordinates θ and φ , as shown in Figure 2.6. More specifically, it gives the power that is radiated or received by a transmitting antenna or by a receiving antenna, respectively, using the angular distribution already referred. That power can vary depending on the direction of radiation, and is measured far away from the antenna terminals. A pattern can be described in three ways:

- **Isotropic pattern:** If an antenna radiates with the same power in all directions, it means that will be a lossless antenna. Those antennas do not exist in the real case though, working only as a reference pattern.
- **Directional pattern:** When an antenna radiates into one or some directions more power than in other directions. Thus, it means that those directions will be preferred for the waves to radiate. Due to the asymmetry of radiation, the pattern varies only with θ (elevation plane), once for φ it will be desirably constant. An example of the three-dimensional pattern is given in Figure 2.7, and the respective polar diagrams are shown in Figure 2.8 and Figure 2.9.
- **Omnidirectional pattern:** When the radiated power is the same along a given plane, - therefore constant - thus concentrating the variation of its pattern along the other plane. An example of the three-dimensional pattern is given in Figure 2.10, and the respective polar diagrams are shown in Figure 2.11 and Figure 2.12.

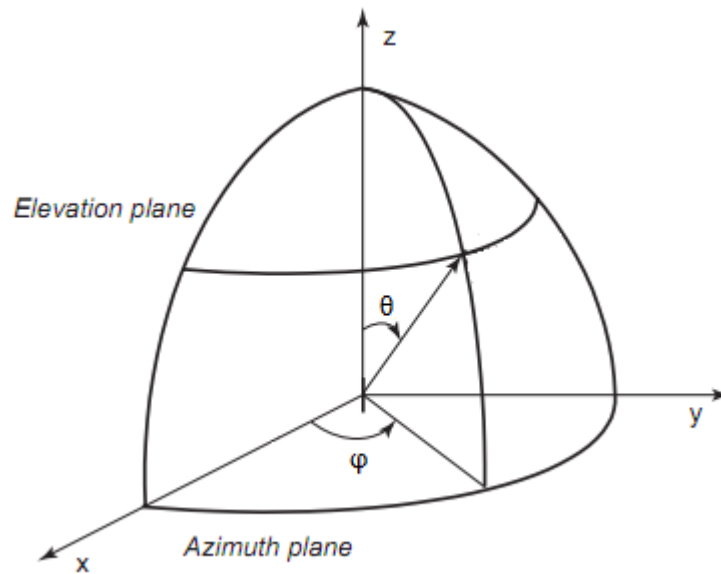


Figure 2.6 - Spherical coordinate system which describes the radiation pattern (adapted from [4])

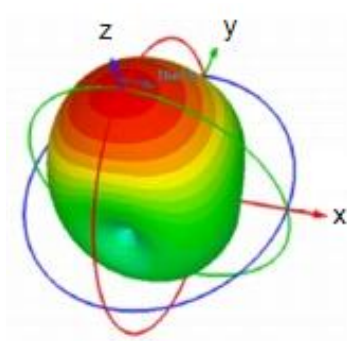


Figure 2.8 - Three-dimensional directional radiation pattern [5]

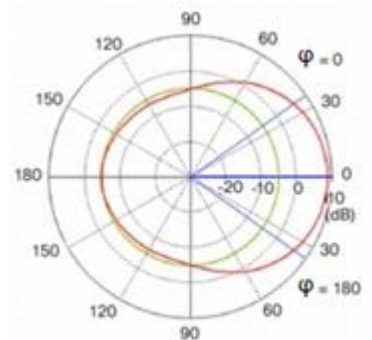


Figure 2.7 - Polar diagram of the azimuth plane radiation pattern [5]

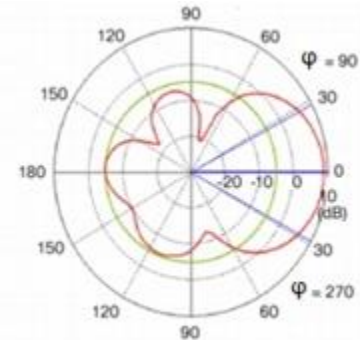


Figure 2.9 - Polar diagram of the elevation plane radiation pattern [5]

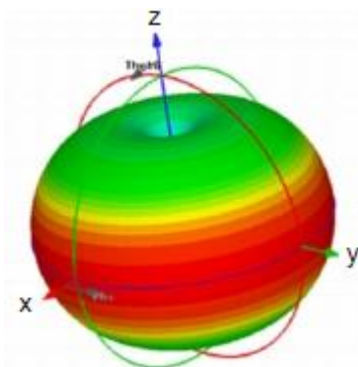


Figure 2.11 - Three-dimensional omnidirectional radiation pattern [5]

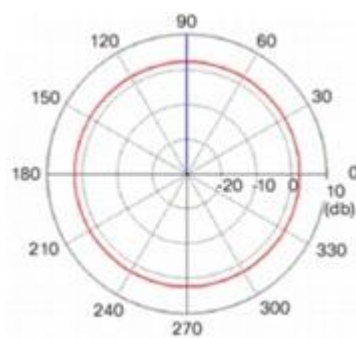


Figure 2.10 - Polar diagram of the azimuth plane radiation pattern [5]

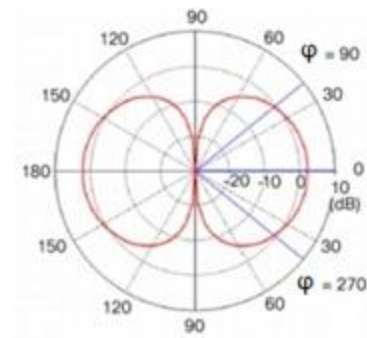


Figure 2.12 - Polar diagram of the elevation plane radiation pattern [5]

Analysing Figure 2.7 one can see that pattern radiates through the Z axis; consequently the polar diagrams of Figure 2.8 shows that for the x-y plane (variation of φ) there is no specific direction of radiation, in contrast with the polar diagram of Figure 2.9 which shows that there is a preferred direction for radiating. Now, analysing Figure 2.10 one can verify that the radiated power is uniform despite of the variation and rotation of the φ angle; therefore the variation of θ angle forms a directional pattern, in contrast to the omnidirectional pattern of the azimuth plane. Again evaluating the respective polar diagrams, it is easy to see that the Figure 2.11 creates a uniform power radiation, and the Figure 2.12 does not create. Finally, both of the three-dimensional graphics are described by colors around its curves; the red represents the peak powers; the yellow refers to intermediate power; and the green represents the lowest powers.

The radiation pattern of an antenna is many times characterised by its lobes (or beams). The part that concentrates more radiation is often referred to main lobe. All the other lobes are called minor lobes, but some of them can have a more specific name though. When some lobe also radiates (although in a second plan) in another direction than the main lobe is called side lobe. At last, there are the so-called back lobes which make an angle of approximately 180° to the main beam. The details of radiation pattern lobes are shown in a partial polar plot (Figure 2.13). [6]

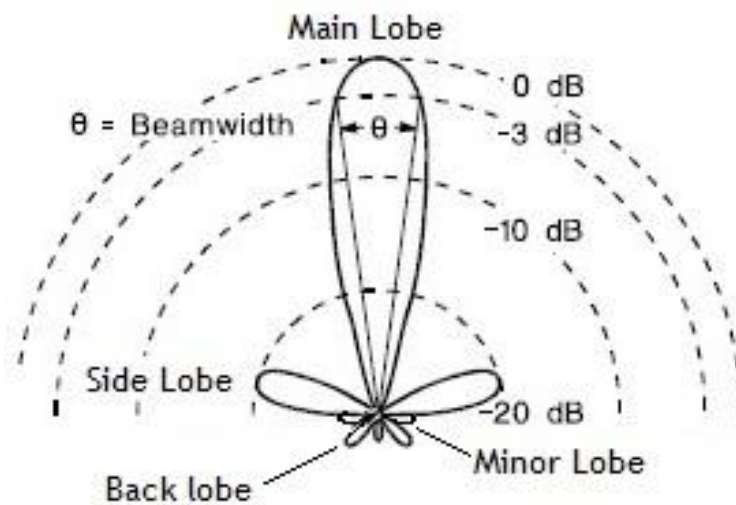


Figure 2.13 - Radiation pattern lobes

2.3.2 Half-Power Beamwidth

The half-power beamwidth (HPBW) is a measure that illustrates the quality of the main beam radiation. That is, if two extreme points of the main beam are defined as the points where the power of radiation pattern decreases by one half (3 dB) from its peak, then the angular distance between those points will give the HPBW (see Figure 2.15 and Figure 2.14). The wider is the angle, the larger will be the main lobe and the thinner will be the side lobe, and vice-versa. These explanations are related with directivity and gain; hence with a small HPBW describing the main lobe, there is a larger directivity and there is a larger gain; consequently more power is concentrated to one specific direction, but the width of the side lobe increases though.

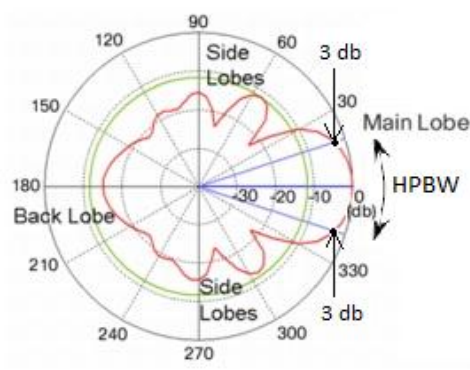


Figure 2.15 - Polar diagram of HPBW (adapted from [5])

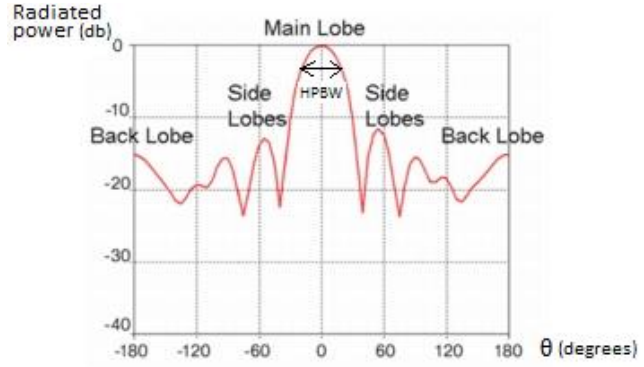


Figure 2.14 - Rectangular diagram of HPBW (adapted from [5])

2.3.3 Directivity

The directivity is a quantity that indicates how powerful is the radiation of an antenna in a specific direction when compared to the radiated power of an isotropic reference. Hence, it is possible to evaluate if the concentration of emitted power will be higher or smaller than the average radiated power in all directions of the antenna. The analytical expression can be defined as [7]:

$$D = \frac{U}{U_0} = \frac{4\pi U}{P_{rad}} \quad (2.4)$$

Where:

D - Directivity;

U - Concentration of radiated power in a specific direction;

U_0 - Concentration of radiated power of an isotropic reference;

P_{rad} - Total radiated power.

Note that U_0 is given by:

$$U_0 = \frac{P_{rad}}{4\pi} \quad (2.5)$$

If there is no directivity in a specific direction, it means that the radiated power will be distributed uniformly in all directions; therefore similarly to the referred isotropic reference. Otherwise, there will be directivity in a specific direction if the concentration of power radiated in that direction is bigger than the one of an isotropic reference. In that case, the directivity will increase with the concentration of power in a direction; thus increasing the gain and decreasing the HPBW [7].

2.3.4 Gain

The gain is expressed as the ratio of the power radiated by an antenna in a particular direction to the power that would be radiated if the supposed antenna was radiating isotropically, emitting the total forward accepted power (at the input terminals) instead of

the total radiated power (at the output terminals), as in directivity. Also, that forward power is divided by a term 4π . Therefore, while in directivity a lossless antenna is implicit; in gain the losses are considered. This is commonly referred as to absolute gain, and it is given by the following formula: [7]

$$G_{abs} = \frac{U}{U_0} = \frac{4\pi U}{P_{in}} \quad (2.6)$$

Where:

G_{abs} - Gain of the antenna;

U - Power radiated in a given direction;

U_0 - Power that would radiate isotropically;

P_{in} - Forward accepted (input) power.

Thus, it means that when the gain is higher than one, the power radiated in the far field will be always higher than the supposed power radiated isotropically. The absolute gain can also be specified in dBi² units, as:

$$G_{dBi} = 10 \cdot \log_{10}(G_{abs}) \quad (2.7)$$

Where:

G_{dBi} - Gain in dBi.

Sometimes, instead of the absolute gain, the relative gain is used to characterise an antenna. The equation is basically the same, though now P_{in} is defined as the power radiated by a reference antenna (or by the main lobe) in its specified direction. In this case the gain is given in dB³:

$$G_{dB} = 10 \cdot \log_{10}(G_{rel}) \quad (2.8)$$

Where:

G_{dB} - Gain in dB;

G_{rel} - Relative gain.

In many cases, the relative gain is referred to a half-wavelength dipole antenna (see section 2.4.1) that serves as a reference; in that case, it means that 0 dBd is equal to

² When the gain of an antenna is measured having as a reference an isotropic antenna. An isotropic radiator has a gain of 0 dBi. Usually, dBi is a positive number.

³ Decibel (dB) is a unit which characterises a measure X as: $X_{dB} = 10 \cdot \log_{10}(X)$; When X refers to a power ratio or measurements. Otherwise, if X refers to a voltage ratio or measurement, its value in dB is given by: $X_{dB} = 20 \cdot \log_{10}(X)$.

2,15 *dBi*. Usually, that kind of antennas work for frequencies lower than 1 GHz and they are the simplest antennas with the least gain of all antennas.

Now, the relationship between gain and directivity is specified by:

$$G = \varepsilon_r \cdot D \quad (2.9)$$

Where:

G - Relative gain or absolute gain;

ε_r - Antenna radiation efficiency;

D - Directivity.

The radiation efficiency comes as:

$$\varepsilon_r = \frac{P_{rad}}{P_{in}} \quad (2.10)$$

Where:

P_{rad} - Total radiated power.

Thus, radiation efficiency parameter gives an idea of how much power is radiated by an antenna when compared to the power that was delivered to the input terminals. The bigger is the radiation efficiency, the bigger is the gain for the same directivity.

2.3.5 Efficiency

Antenna efficiency is a parameter that measures the losses at input terminals of an antenna. As explained in section 2.3.4 P_{in} is the power of an antenna at its input terminals and is defined by: [7]

$$P_{in} = P_{rad} + P_{losses} \quad (2.11)$$

Where:

P_{losses} - Power that an antenna loses while the EM waves are being transported to its output terminals.

Therefore, only the power P_{rad} will be radiated. Thus, the antenna total efficiency can be calculated as:

$$e_0 = \varepsilon_r e_r \quad (2.12)$$

Where:

e_0 - Antenna total efficiency;

ε_r - Antenna radiation efficiency (see equation (2.10));

e_r - Reflection efficiency.

The latter is given by:

$$e_r = 1 - |\Gamma|^2 \quad (2.13)$$

Where:

Γ - Reflection coefficient (see section 2.3.6).

The efficiency plays an important role in the classification of antenna gain.

2.3.6 Scattering Parameters

Scattering parameters (or S-parameters) are a very useful system to characterise the incident and reflected waves in a linear two-port structure. Figure 2.16 shows the respective network.

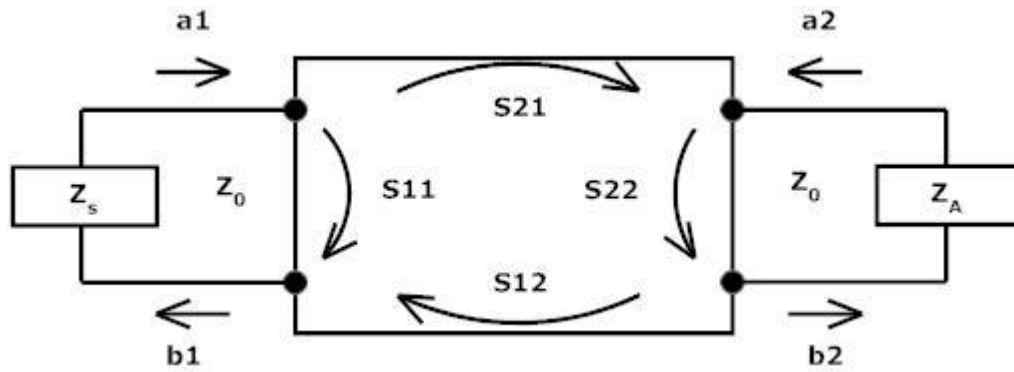


Figure 2.16 - Two-port network constituted by S-parameters

The S-parameters are defined as follows:

$$S_{11} = \left. \frac{b1}{a1} \right|_{a2=0} \quad (2.14)$$

$$S_{22} = \left. \frac{b2}{a2} \right|_{a1=0} \quad (2.15)$$

$$S_{21} = \left. \frac{b2}{a1} \right|_{a2=0} \quad (2.16)$$

$$S_{12} = \left. \frac{b1}{a2} \right|_{a1=0} \quad (2.17)$$

Where:

S_{11} - Input reflection coefficient;

S_{22} - Output reflection coefficient;

S_{21} - Forward transmission gain;

S_{12} - Reverse transmission gain;

a_1 - Wave of incident power on the input of the network;

a_2 - Wave of incident power on the output of the network;

b_1 - Wave of reflected power from the input of the network;

b_2 - Wave of reflected power from the output of the network.

The reflection coefficient of the network as a whole is defined as the ratio of the amplitude of the reflected wave to the amplitude of the incident wave. When applied to a transmission line, it comes as:

$$\Gamma = \frac{Z_A - Z_0}{Z_A + Z_0}, \quad -1 \leq \Gamma \leq 1 \quad (2.18)$$

Where:

Γ - Reflection coefficient;

Z_A - Impedance of the load;

Z_0 - Impedance of the transmission line.

Note that for $\Gamma = 1$, Z_A is infinite and there is an open-circuit; otherwise, for $\Gamma = -1$, Z_A is zero and there is a short-circuit. The perfect situation occurs for $\Gamma = 0$, when there are no reflections from the transmission line, and subsequently the maximum amount of power can be provided to the load. If the reflection coefficient formula is applied to S_{11} , the load will be now given by the input of the network; so the input reflection coefficient comes as:

$$\Gamma_{in} = S_{11} = \frac{Z_1 - Z_0}{Z_1 + Z_0} \quad (2.19)$$

Where:

Γ_{in} - Input reflection coefficient;

Z_1 - Input impedance at port 1.

Likewise, if the reflection coefficient is applied to S_{22} , the output reflection coefficient comes as:

$$\Gamma_{out} = S_{22} = \frac{Z_2 - Z_0}{Z_2 + Z_0} \quad (2.20)$$

Where:

Γ_{out} - Output reflection coefficient;

Z_2 - Output impedance at port 2.

Therefore, taking into account that S_{11} and S_{22} are defined as reflection coefficients, those parameters can be used to measure the reflections at the input and output ports respectively. In the practical case, S-parameters are measured in dB, and they can be

measured in an instrument called vector network analyser (see Figure 5.1). Return loss (RL) is the parameter which is used to measure the ratio of both S_{11} and S_{22} in dB, depending on the port. Equation (2.21) gives the return loss for S_{11} (the formula also applies to S_{22}).

$$RL_{dB} = -20 \cdot \log |S_{11}| \quad (2.21)$$

Where:

$|S_{11}|$ - Magnitude of S_{11}

Note that usually RL is a negative number; the more negative RL is, the more power is delivered to the load and less is reflected. Thus, that indicates the source and characteristic impedances are matched to the load (see section 2.3.7) for more details about impedance matching).

Another parameter which measures the transmission gain in dB is insertion loss (IL), given by equation (2.22). Basically, it measures the losses in transmission line of an antenna.

$$IL_{dB} = -20 \cdot \log |S_{21}| \quad (2.22)$$

The optimum value for IL is 0 dB, which means that no power is reflected and so the total power generated by the source is given to the load. Although in the practical case transmission lines are always submitted to losses.

Smith charts are the way to represent RL_{dB} and IL_{dB} . Fortunately, vector network analysers plot them in a way to find a matching between transmission lines and loads of antennas.

2.3.7 Voltage Standing Wave Ratio

Voltage standing wave ratio (VSWR) is a parameter that measures the matching between an antenna and a transmission line. Essentially, it states the power that an antenna will get from a transmission line, in order to be able to radiate as much as possible of that received power. Usually, VSWR is calculated as the ratio of the maximum amplitude to the minimum amplitude of the voltage of a standing wave⁴. It comes as:

$$VSWR = \frac{V_{max}}{V_{min}} \quad (2.23)$$

Where:

V_{max} - Maximum amplitude of the voltage of a standing wave in volts (V);

V_{min} - Minimum amplitude of the voltage of a standing wave in volts (V).

VSWR is also given by the following equation:

⁴ A standing wave is a wave which is created by the overlapping of a forward traveling wave and a reflected wave traveling in opposing directions; this creates a barrier for the propagation of energy.

$$VSWR = \frac{1 + |\Gamma|}{1 - |\Gamma|}, \quad |\Gamma| \leq 1 \text{ and } VSWR \geq 1 \quad (2.24)$$

Where:

$|\Gamma|$ - Magnitude of the reflection coefficient.

VSWR is also given by equation (2.25), because S_{11} is also a reflection coefficient.

$$VSWR = \frac{1 + |S_{11}|}{1 - |S_{11}|} \quad (2.25)$$

Where:

$|S_{11}|$ - Magnitude of the input reflection coefficient.

Note that a good value of VSWR (low value) means that an antenna is well matched, and subsequently the amount of power that an antenna receives from a transmission line is very satisfactory; otherwise, a high VSWR value means that an antenna is mismatched, and then the loss of power delivered to the antenna will be very high. In this case, an antenna will not radiate power, once the wave is reflected back and will not approach the antenna terminals [8].

Technically speaking, VSWR is always greater than or equal to one. A good matching can be found when $VSWR < 2$, and an ideal matching is given by $VSWR = 1$, where there is no reflected power. In Table 2.2, the different values of VSRW are compared when related with the reflection coefficient, return loss, and mismatch loss.

Table 2.2 - VSWR in numbers

VSWR	Reflection coefficient	Return loss (dB)	Reflected power (%)	Mismatch loss (dB)
1	0	∞	0	0
1,5	0,2	13,979	4,000	0,177
2	0,333	9,542	11,112	0,512
2,5	0,429	7,36	18,365	0,881
3	0,5	6,021	24,998	1,249
4	0,6	4,437	36	1,938
6	0,714	2,923	51,015	3,1
10	0,818	1,743	66,942	4,807
20	0,905	0,869	81,865	7,413
40	0,951	0,434	90,490	10,214
100	0,98	0,174	96,073	14,066
∞	1	0	100	∞

2.3.8 Polarisation

When an antenna radiates EM waves in a certain direction at any point in the far field, its characterisation is given by a figure that traces out the magnitude of the electric field vector along the propagation time. This property is called polarisation. Basically, it can be described as a measure of how the EM waves are orientated along its emission. If a polarisation is not settled, one can assume that the direction of the maximum gain will also be the one for the polarisation [7, 9]. There are three types of polarisation:

- Linear polarisation
- Circular polarisation
- Elliptical polarisation

The linear polarisation is due to the linearity of the electric field vector. When the latter at a certain point in the far field is always described by a line travelling in a single direction as a function of time, it means that its polarisation is linear. On the other hand, the antenna can be horizontally or vertically polarised when linearly polarised, depending how oriented the field is in order to the ground. Take note that for different types of linear polarisation, different antennas are not able to communicate. Concerning to the circular polarisation, its characteristics are part of an antenna if the electric field vector outlines a circle as a function of time at a certain point in the far field. At last, the elliptical polarisation describes an antenna when its electric field vector at a far field point is such that traces elliptical curves constantly with time [7]. Moreover, both the circular and elliptical polarisations are characterised for being right-hand (RH) or left-hand (LH) polarised, depending on the sense of the field; if the field is flowing in the clockwise direction, the field will be right hand polarised; otherwise it will be left hand polarised. Examples of circular and linear polarization are shown in Figure 2.17 and Figure 2.18, respectively. Meanwhile, as the purpose of this thesis is to give attention to broadband feeds, it means that the circular polarisation will be completely focused, in order to be applied to satellites of Non-geostationary Earth orbit (see section 2.8.1). Therefore, the polarisations that will be used are the right-hand circular polarisation (RHCP) or the left-hand circular polarisation (LHCP).

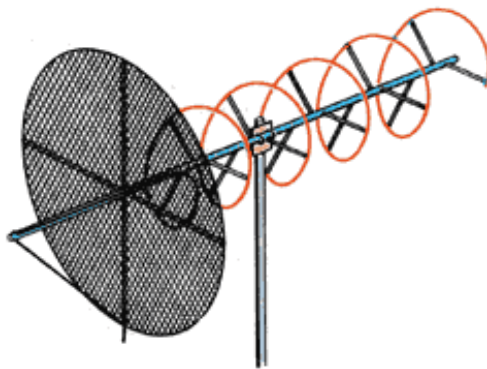


Figure 2.17 - Helical antenna with RHCP [8]

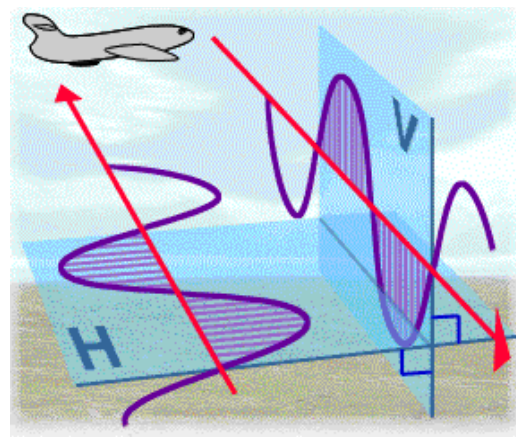


Figure 2.18 - An airplane antenna emitting [9]

2.3.9 Input Impedance

The input impedance of an antenna is the measure that establishes the ratio of the voltage to the current at its input terminals. Basically, those terminals are a transition between the transformation of the electric current produced by the transmitter and the EM waves that will be radiated, work as a load to the transmission line; therefore, the input impedance is a characteristic that describes and gives an idea of how powerful the radiation will be, once it is possible to calculate the maximum power that is transmitted to the antenna before emitting the EM waves. The general expression of input impedance is given by [7]:

$$Z_{in} = R_A + jX_A \quad (2.26)$$

Where:

Z_{in} - Input impedance in ohms (Ω);

R_A - Antenna resistance in ohms (Ω);

X_A - Antenna reactance in ohms (Ω).

All these values are pointed to the input terminals of the antenna. R_A is:

$$R_A = R_L + R_r \quad (2.27)$$

Where:

R_L - Loss resistance in ohms (Ω);

R_r - Radiation resistance in ohms (Ω).

As shown above, input impedance is the sum of a real number and of an imaginary number. The first specifies the power that antenna radiates or the power that antenna takes in, while the imaginary part specifies the power that is not radiated by the antenna, thus retained not far away from its terminals.

Frequency (also the wavelength) makes the impedance vary consonantly its value is high or not. For lower frequencies (higher wavelengths) the length of the transmission line is not significant when compared to wavelength, so the result is a short line. Although for higher frequencies where the transmission line is slightly a big fraction of a wavelength, it can be a problem because the input impedance will be influenced in a large scale by the length of the transmission line. Therefore, the term impedance matching becomes important, because in this case the length of a transmission line is not significant when compared to the wavelength. The input impedance of an antenna will be matched with a transmission line if both impedances are the same ($Z_A = Z_0$). The matching is measured by a parameter called VSWR, which is focused in section 2.3.7 . If an antenna is mismatched, the loss of power can be very high, because the power generated by the source will be reflected back.

As a measure related with power, input impedance is a crucial quantity for the power that an antenna will receive. Thus, as a definition, a maximum power will be delivered from

the source to the antenna, if the input impedance is equal to the conjugate of the impedance generated by the source $Z_A = Z_S^*$. Therefore, no power will be transmitted when Z_A is much smaller or much superior than Z_S . The respective circuit is shown in Figure 2.19.

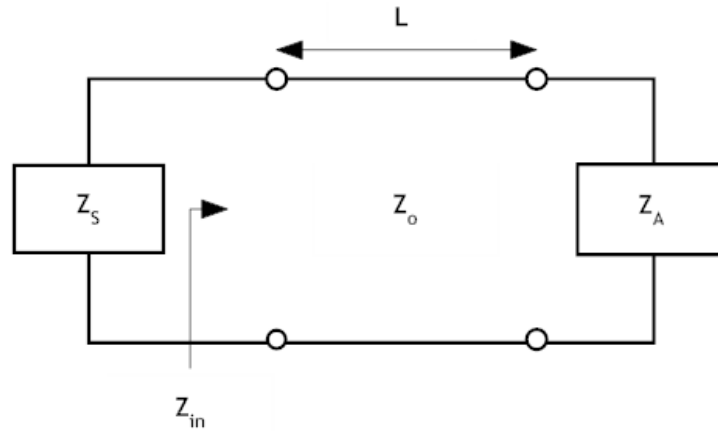


Figure 2.19 - Circuit representing input impedance at the entrance terminals of the transmission line

2.3.10 Bandwidth

The term bandwidth specifies the range of frequencies which an antenna can achieve, in order to obtain a desirable behaviour of a certain characteristic. It is classified as the first required condition before building an antenna, because it is a measure of how acceptable the performance of an antenna can be. However, as a range, two boundaries define the lower and upper frequency limits, and the ratio of its size to the centre frequency as a percentage define the percent bandwidth for a narrowband antenna - thus occupying a small space quantity on the RF spectrum - given by equation (2.28); otherwise, for a broadband (or wideband) antenna the bandwidth is defined as the ratio of the upper to lower frequencies as written in equation (2.29). Both expressions are analytically represented as [7, 10, 11]:

$$B_f = \frac{f_H - f_L}{f_C} \times 100 \quad (2.28)$$

$$B_r = \frac{f_H}{f_L} \quad (2.29)$$

Where:

B_f - Fractional bandwidth in Hz percentage;

B_r - Bandwidth ratio;

f_H - Upper frequency in Hz;

f_L - Lower frequency in Hz;

f_C - Centre frequency in Hz;

For example, in equation (2.28) if a result of B_f could be 3% that means the difference between the working frequencies would be 3% of the centre frequency; while in equation (2.29) with a B_r of 5 it means the upper frequency is 5 times bigger than then lower.

Usually, the described parameters of an antenna may have a satisfactory value of those at the centre frequency; therefore a bandwidth involving it, for which those parameters are able to have a good performance. In fact, all the parameters can be influenced by frequency in a different way, what gives a different meaning to the bandwidth of each. Especially analysing the radiation pattern (see section 2.3.1) and input impedance (see section 2.3.9) bandwidth differences, the useful bandwidth of a designed antenna can be related to both, despite of the disparity on those differences. In some cases the satisfactory bandwidth for radiation pattern goes above the one for input impedance, or vice-versa. Also, that happens to more parameters such as: radiation efficiency and input impedance; beamwidth and gain; among others. So, the important conclusion to be taken is that for the same frequency or for a certain bandwidth of frequencies, a different performance can be obtained when several parameters are tested. An example of a VSWR bandwidth is shown in Figure 2.20 (see section 2.3.7), when a bandwidth is stated between the limits f_L and f_H .

For a thin antenna dipole (see section 2.4.1), input impedance is the limiting factor, because radiation pattern is not sensitive to frequency; thus it makes more sense to take advantage of radiation pattern properties to establish the narrow bandwidth; for intermediate length antennas both radiation pattern and input impedance properties work as limiting factors - 2:1⁵ bandwidth ratios are reached; and for other antennas, such as frequency independent antennas (see section 2.6), large bandwidths are required - 40:1 bandwidth ratios are normally achieved. [7, 11, 12]. These referred antennas will be analysed as the main topic of this thesis, and they are also known as broadband antennas (see section 2.5).

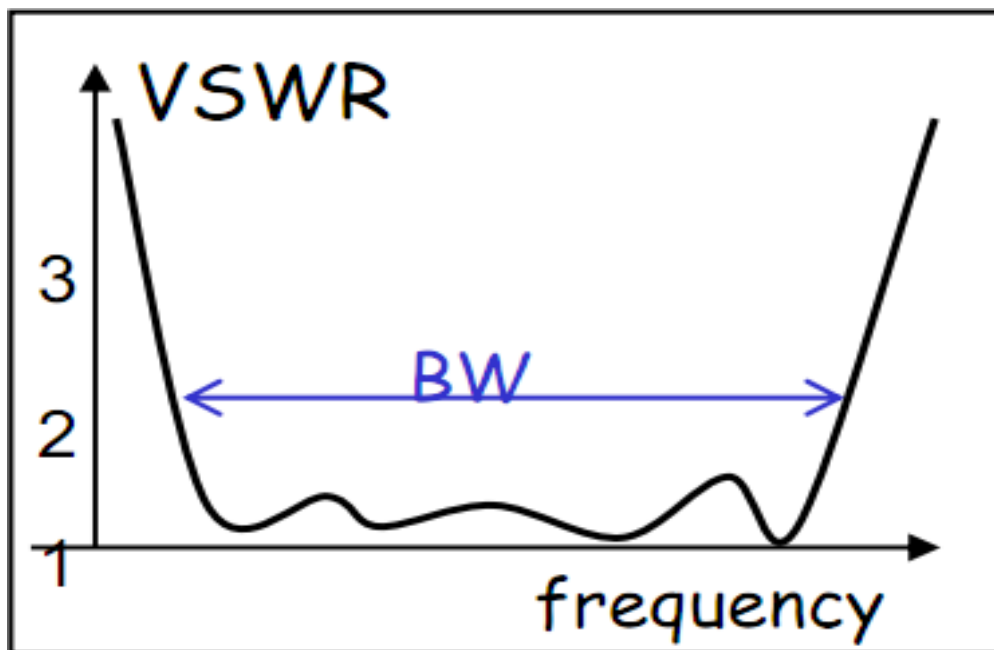


Figure 2.20 - Frequency bandwidth for VSWR parameter

⁵ For any f_L : f_H bandwidth ratios, the upper frequency is f_L times greater than the lower f_H .

2.3.11 Reciprocity

It is the principle which states that an antenna may send or receive EM waves in an equal manner. That is, the characteristics of an antenna must remain the same while receiving or radiating. Thus, reciprocity can also be measured analysing the radiation pattern of an antenna, which again, may look the same while transmitting or receiving RF waves. S-parameters are also a notable case of reciprocity.

2.4 Types of Antennas

There are several types of antennas which were developed since the past times due nowadays. In this section, a study of the different antennas based on the parameters described previously in section 2.3 is made. The following types of antennas are presented: Wire antennas; aperture antennas; microstrip antennas; reflector antennas; and travelling wave antennas [13].

2.4.1 Wire Antennas

Wire antennas are between the most used antennas. Basically, they are very simple and cheap, with linear or curved forms. There are mainly three shapes which are characterised by those forms. They are:

- Linear dipole antennas: defined by a straight wire fragmented in two sections, within a fed usually between them. They can be seen on the mobile phones and they can work as a FM radio receiver.
- Loop antennas: It can be a circular, square, triangle, rectangular or elliptical form. They are used as AM radio receivers for example. In the past they were used in pagers.
- Helical antennas: with a shape defined by helices, similarly to a spring shape. Those antennas are used for space telemetry through VHS satellite transmission.

In linear dipole antennas the simple straight wire has size L . The shorter is the size of the wavelength (λ) dipole, the shorter will be the power of its radiation in a given direction, and consequently the gain. Therefore, different types of dipoles can characterise a linear dipole antenna, and they are generally fed at the centre. Dipoles are also linearly polarised; almost always horizontally polarised (the case of broadband dipoles) for a high frequency of operation, and vertically polarised for a low frequency. Figure 2.21 represents a typical linear dipole with a certain λ . Some of the most used dipoles are the vertical polarised, such as: short dipoles, quarter-wavelength dipoles, and half-wavelength dipoles.

The short dipole is one of the simplest antenna structures, and it applies to Figure 2.21 when the length L is very small compared to λ . There is also no specific directivity in its radiation pattern; therefore it is an omnidirectional antenna with a HPBW of 90° . The input impedance of short dipole has higher loss resistance than radiation resistance, thus the radiated power is low, and its efficiency is very small. VSWR bandwidth is very small; about 2% of the operating frequency.

Quarter-wavelength dipoles have mainly the same characteristics as the short dipole, but the length of its wire is about a quarter-wavelength of the operating frequency. This antenna is omnidirectional with an almost 90° HPBW. In practice, this is the shortest antenna which is able to radiate due to the help of a ground reflection (or an artificial ground plane - see section 3.2.2) that acts as a mirror. Not that this condition is important at lower frequencies. VSWR bandwidth is about 5% of the operating frequency.

Half-wavelength dipoles have the same properties as the other dipoles, but in this case the length of its wire is not so small when compared to the wavelength; therefore its length is equal to a half wavelength at the working frequency. Again Figure 2.21 serves as a reference. In this case, the directivity is higher than the one for the short dipole; consequently its HPBW is lower. Input impedance has a lower component of loss resistance than to radiation resistance, which enables a better matching. Also the reactive component is low, and it can be eliminated if instead of a half-wavelength there is a $0,48\lambda$.

Note that there more types of dipoles as full-wavelength dipole or broadband dipoles. They can operate at a higher frequency than the referred dipoles, and they also have a much better matching; then a low VSWR. Although, they are not suitable for high frequency usage, because their VSWR bandwidth is very narrow

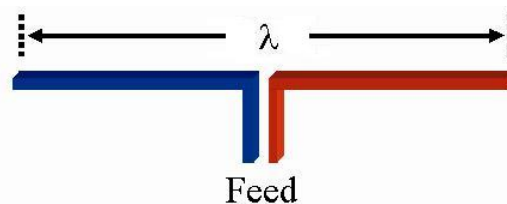


Figure 2.21 - The wavelength of a dipole antenna [14]

Typical loop antennas, as referred previously, have a circular or a square shape (small loop antennas). They have very low efficiency and low gains, and polarization is horizontal for both, usually with an almost omnidirectional HPBW. The most of loop antennas operate in HF, VHF, and UHF bands (see section 2.2) [13]. Loop antennas are divided into two groups: electrically small and electrically large. Electrically small loops are characterised for a very small wavelength (usually about $\lambda/10$), while electrically large loops are characterised for working in a related way to the dipoles of full-wavelength or more. As long as the electrical size of a loop increases, the radiation resistance gets higher and a better matching with a transmission line is obtained.

Small loops are mainly used as receiving antennas. Due to a low radiation resistance when compared to loss resistance, losses are very high; enabling a high inefficiency and consequently a lot of received power is wasted. The radiation pattern is often comparable to the very small wavelength dipole.

Large loops are frequently used as directional antennas, forming arrays⁶ characterised by higher gains and directivities, and such sequence of (circular) loops form the so-called helical

⁶ Constituted by multi-elements (individual antennas), in order to form a new single configuration with higher electrical size. Each element has its own current. The sum of all currents is treated as in a vector. Therefore, arrays have high gain suitable for long distance communications.

antennas (see ahead in this subsection). They are characterised for having a high directivity and gain.

Helical antennas are displayed as a helix and usually they consist in a wire connected to a coaxial cable and a ground plane, and they are fed at one end and opened at the other. The polarisation is elliptical and the typical HPBW is of 50° . The gain can be as high as 10dB for an axial mode helix, shown in Figure 2.17. They are a type of broadband antennas (see section 2.5), displayed as series of loops forming a coil shape.

2.4.2 Aperture Antennas

These types of antennas are utilised at high frequencies. Aperture antennas largely depend on their aperture, because this property is directly related to gain. A notable example of an aperture antenna is the horn antenna. Although another well-liked aperture antenna is the slot antenna. Both are described as follows: [13]

- Horn antennas: Used mainly in UHF (Ultra high frequency) frequencies. High gains are provided due to its high directivity. Thus, bandwidths of 20:1 can be achieved. The larger the horn is the higher the directivity will be. There are low losses when D is equal to G. Horn antennas can be used as a feed in reflector antennas; they are also used in aircraft for example.
- Slot antenna: Metal plate which has a hole or slot within it. Usually, frequencies up to 24 GHz can be reached. They are often used at UHF and microwave frequencies. Another interesting property of these antennas is their almost inexistent directivity, allowing omnidirection radiation patterns. They also have linear polarisation.

2.4.3 Microstrip Antennas

Microstrip antennas or microstrip patch antennas are usually very cheap and small, with an easier manufacture. They are printed directly onto a printed circuit board (PCB), and they are made of a metallic patch with a rectangular or circular shape, embedded on a grounded substrate. Microstrip antennas have a linear polarisation and their gain is about 6 dB. Typically narrowband, rectangular microstrip antennas work at an average frequency of 100 MHz. Despite of that, they can be found on the mobile phones [9].

2.4.4 Reflector Antennas

Reflector antennas also known as reflector antennas or satellite dish antennas are a specific type of antennas for long distance communications. Although, the name parabolic antenna is probably the most known. The constitution of this antenna is based on two main components:

- Parabolic reflector: It acts as a reflector (mirror) for the waves that go across their dish.
- Feed: It is the front part of a parabolic, which acts as a focal point. In fact, the antenna itself is located here.

The parabolic reflector has a shape of a parabola because all the EM waves transmitted from the feed to the dish will be reflected into the same direction, whatever the angle of incidence is. Because of that, the directivity of such parabolic antenna is very high, and consequently the gain follows. Therefore, typical gains of 40 dB are achieved. The wider the dish is the wider the gain will be. It also means that the aperture should be larger; very wideband bandwidths are achieved then. Another property that results is the low cross polarisation, because the reflected waves are in phase. Often a horn antenna works as a feed of circular aperture, to allow the circular polarisation, required for parabolic antennas.

As the main task of this thesis is to make a broadband feed for a reflector antenna, this is an important background subject. Despite of the wide usage of horn antennas as a feed, another antenna was required for the work specified. The choice of the planar equiangular spiral antenna was chosen though. A parabolic antenna is shown in Figure 6.1.

2.4.5 Travelling Wave Antennas

Travelling wave antennas are characterised by a current varying continuously along its structure. Another interesting property that makes travelling wave antennas mostly appreciated is the matching of its load resistance (Z_A) to the characteristic impedance (Z_0); therefore, no VSWR factor exists and subsequently no reflected waves. Such antennas are commonly used in high frequency bands. Examples of travelling wave antennas are: [9]

- Yagi-Uda antenna: These antennas are widely known to the layman. They are seen practically everywhere on the roofs of buildings. For such a simple manufacture, the gains achieved are great. The main disadvantage is the low bandwidth coverage.
- Helical antenna: Although this is a typical wire antenna, the most used helical is a travelling wave antenna. These antennas are described for having high bandwidths due to its circular polarisation. Input impedance is commonly real; thus enabling low losses of power. The pointed direction concentrates the most of the radiation pattern.

2.5 Broadband Antennas

In a very simplified way, a broadband (or wideband) antenna can be defined as an antenna which has a wide bandwidth. Therefore, this means that an ample range of frequencies are covered, enabling an antenna to work throughout a large spectrum. More specifically, a more effective explanation establishes that a broadband antenna has no important changes in the radiation pattern and impedance occurring over an octave ($f_H = 2 \times f_L$) or more. Usually, for a narrowband antenna, high resonance⁷ characteristics are very

⁷ Resonance is the property that an object presents when its natural frequency is stressed along time, creating large amplitude oscillations by accumulating and adding small amounts of external energy in time with the natural frequency, thus generating vibration.

common along its properties once the standing waves⁸ describe the propagation process. Meanwhile, for a broadband antenna, travelling waves⁹ characterise the propagation pattern.

2.6 Frequency Independent Antennas

2.6.1 Introduction

A frequency independent antenna is a structure where the radiation pattern, impedance properties and polarisation are frequency independent only if the antenna configuration is specified completely by angles [8]. Also, the referred parameters remain virtually unchanged over very large bandwidths [15]. The use of this process can only be applied taking into account that if the dimensions of a conducting antenna vary in linear proportion with the wavelength, its performance won't change unless for all measurements of length a change of scale occur [16]. Unlike frequency dependent antennas where the fundamental properties are based on its shape and dimensions expressed in wavelengths, frequency independent antennas have nothing to do with those wavelength expressions. This is applied here because wavelength is inversely proportional to frequency, so normally antennas present frequency dependent features.

Powerful broadband antennas work based on frequency independent concepts. The frequency independent theory is applied when the dimensions of an antenna are infinite, however, in the practical case, it doesn't really happen once we must have finite dimensions [13, 16-18]. Therefore, using all the above described techniques, another tip is required for a practically independent performance. Thus, it is possible to overcome this problem just by defining at least one arm length of finite size [5]. This process is described ahead in detail. Meanwhile, as long as the distance from the terminals increases, the current that flows through an infinite antenna structure (in the real case should be finite with infinite antenna properties) must decrease until its negligibility occur. If the opposite could happen, a truncation would result in a radial effect on the radiation pattern; however, that results in a lower cut-off frequency above which its radiation properties reflect those of the infinite structure and in an upper cut-off frequency limited to frequencies for which the length of the feed transmission line is bigger than the highest obtained frequency under 8 units - $\lambda/8$ - usually represented by a small point; therefore, we obtain ratio bandwidths of about 40:1 [6]. Examples of frequency independent antennas are the log-periodic (see Figure 5.5); the conical spiral; or the equiangular spiral antenna. As a final point for the introductory analysis, the so-called spiral antennas are the ones that are mostly based on the frequency independent principles.

2.6.2 Analytical Description

Now, let's focus on the analytical description of the problem itself. Looking at the shape of a typical frequency independent antenna, the best way to describe the geometry of its

⁸ Defines a wave which results from the combination of two waves that travels in opposite directions, sharing the same amplitude and the same frequency. There is no transmission of energy along its extent.

⁹ When waves are travelling in the same direction, its interference creates a travelling wave which generates energy that propagates in a specific direction and with a specific speed.

curve is to use the spherical polar coordinates system, due to a scalar variation of the angle of rotation around a fixed point that is connected to the surface or edge of the curve, defining a radius. The latter defines a distance r that varies along the surface or edge as a function of the angle ϕ as follows:

$$r = F(\theta, \phi) \quad (2.30)$$

Where:

r - Radius or distance that varies along the surface or edge in metres;

θ - Inclination or polar angle in degrees or radians;

ϕ - Azimuth angle, degrees or radians.

Those properties define the planar structure of this antenna, and the central terminals are infinitely close to the origin considering that each one is symmetrically represented along $\theta = 0$.

If a factor K of scaling is used to keep the electrical dimensions of the structure when an antenna is scaled to another frequency, it means that the new surface will be:

$$r' = K \cdot r = K \cdot F(\theta, \phi) \quad (2.31)$$

The factor K represents the ratio of the hatched area to the double hatched area when a rotation over an angle C occurs, as shown in Figure 2.22. Also, it is not possible to make a translation of the geometry combined with the scaling of the geometry size, because the terminals of both structures (2.30) and (2.31) are located at the origin; and it is not possible to make a rotation in θ because now the terminals are placed along $\theta = 0$. Meanwhile, we should note that K is related to C , although K and C are independent of θ and ϕ . The new expression considering the angle of rotation C comes as:

$$K \cdot F(\theta, \phi) = F(\theta, \phi + C) \quad (2.32)$$

Using the latter, if we differentiate it in order to ϕ and C , we will obtain similar expressions, and so we obtain a new expression where the left part is independent of θ and ϕ :

$$\frac{1}{K} \frac{dK}{dC} = \frac{1}{r} \frac{\partial r}{\partial \phi} \quad (2.33)$$

Where $\frac{1}{K} \frac{dK}{dC} = a$.

Finally, the general solution of the differential equation (2.31) as defined by Rumsey [19] is:

$$r = F(\theta, \phi) = e^{a \cdot \phi} \cdot f(\theta) \quad (2.34)$$

Where:

$f(\theta)$ - Arbitrary function.

The equation (2.34) represents the description of an independent frequency structure.

It can be realised that the radiation pattern is modified azimuthally by the angle C and for an infinite positive K is also modified and rotated by C in ϕ with frequency. Although, the pattern shape is not changed, what let us affirm that the impedance and radiation pattern are independent of frequency, as written before.

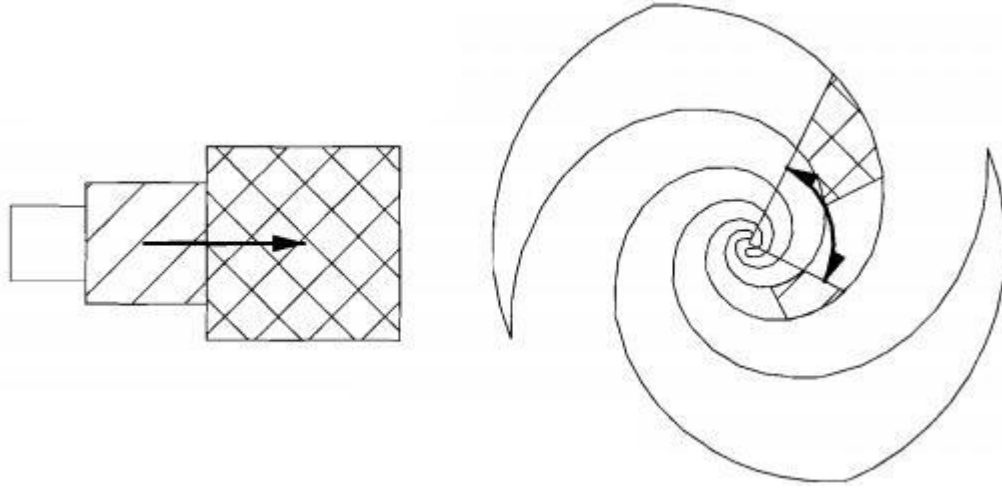


Figure 2.22 - Translation and rotation processes to scale a frequency independent antenna [17]

2.7 Planar Equiangular Spiral Antenna

The planar equiangular spiral antenna (PESA), also called log-spiral antenna, is a frequency independent antenna, thus completely described by angles. Usually, bandwidth ratios over 10:1 can be reached. The shape of an equiangular spiral antenna curve is shown in Figure 2.23 and is defined by [16] using the following equation:

$$\rho = \rho_0 e^{a\phi} \quad (2.35)$$

Where:

ρ - Radial distance from the centre of the spiral to the point angle ϕ ;

ρ_0 - Initial inner radius;

a - Tightness of the spiral arm;

ϕ - Rotation angle with respect to x axis.

The total length of the spiral is given by [13]:

$$L = (\rho - \rho_0) \sqrt{1 + \frac{1}{a^2}} \quad (2.36)$$

Where:

L - Total length of the spiral

The usage of a single spiral itself is not properly thought; therefore, to create an antenna which is able to conduct and work correctly, the definition of two spiral curves is required to characterise one fixed arm (spiral) length in order to obtain a finite size structure. The outer and inner radii of both spirals are named as ρ_1 and ρ_2 . On the other hand, in order to have a balanced antenna with infinite length, another two spirals ρ_3 and ρ_4 define the second arm. It comes as:

$$\rho_1 = \rho_0 e^{a\theta} \quad (2.37)$$

$$\rho_2 = \rho_0 e^{a(\theta-\delta)} \quad (2.38)$$

$$\rho_3 = \rho_0 e^{a(\theta-\pi)} \quad (2.39)$$

$$\rho_4 = \rho_0 e^{a(\theta-\pi-\delta)} \quad (2.40)$$

Where:

δ - Rotation of a fixed angle along the spiral arms in degrees.

Note that:

$$K = e^{a\delta} = \frac{\rho_2}{\rho_1} = \frac{\rho_4}{\rho_3} \quad (2.41)$$

Where:

K - Width along the defined radius.

Usually, K parameters are between 0,375 and 0,97 and a is between 0,2 and 1,2. Although, a balanced PESA is defined mainly by its arm length, by ρ_0 , and by K . The latter must be lower than 1. Finally, the four spirals developed an equiangular spiral antenna, can be plotted as in Figure 2.22.

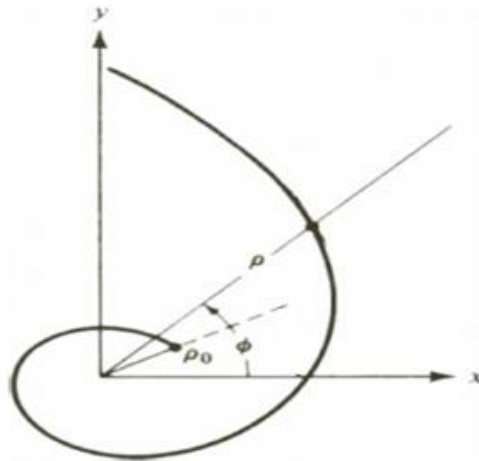


Figure 2.23 - Planar Equiangular Spiral antenna curve [13]

2.7.1 Planar Equiangular Spiral Antenna Feeding

The infinit balun method is one of the two ways to feed the terminals of a slot antenna, which is a notable case of PESA. It is simply described by fixing or soldering a coaxial cable to the metal arms of the antenna. This method is described by keeping the properties of impedance and radiation pattern as infinite. The value of K and a parameters depend on the length of the coaxial cable. The radiation pattern created by this method is of 20:1 bandwidth sometimes. The constitution of a PESA PCB is shown in Figure 3.9.

2.8 Satellite Systems

Satellite systems are one of the most powerful structures for establishing communications quickly and with high quality between any specified world locations. There are several varieties of satellite communication (SATCOM) systems as follows [20]:

- Broadband satellite systems
- Personal communication system
- Navigation
- Domestic
- Military
- Regional
- International
- Experimental
- Meteorology

SATCOM are based upon two segments:

- Ground segment: The part which is located on the Earth as a network control centre; the place for the ground station itself, which has all the necessary engines to transmit and receive what is modulated or demodulated by antennas, respectively. Both processes use digital communication suitable for the transmission of the digital signals of voice (telecommunications signals), video (television broadcasting¹⁰), and data (internet for example). Regardless of its importance on SATCOM, the way that process is done it is not relevant for the purpose of this thesis.
- Satellite segment: The part which is located on the space. Basically, works as a conjunction of the satellite antenna communicators within the satellite control centre, which does the maintenance of the satellite as a whole. The transmission and receiving of data is mainly done by antennas installed on the structure (called transponders), which receive, amplify and retransmit a signal, allowing its transmission in a different frequency than the one which was received. Although, that process is also supported by antennas on the main satellite panel to set up the connection between antenna on the ground segment and transponders. Also, several

¹⁰ One satellite transmitting for millions of receivers.

components installed on a satellite control centre allow the tracking of a satellite on a ground station through its location on an orbit (see section 2.8.1).

SATCOM can be either one way or bi-directional. An example of one way communication is the broadcast of radio and television from a ground station transmitting to several receiving ground stations through a satellite. On the other hand, the usage of transponders in satellites enables bi-directional communication between a satellite and a ground station. When a ground station transmits data to a satellite, the link is called uplink; otherwise, when a ground station receives data from a satellite station, the link is called downlink. Examples of bi-directional communications are the mobile phone links or the telephone and fax long distance connections. The communication process is illustrated in Figure 2.24, where the dashed lines when applied represent the existence of a bidirectional communication [20].

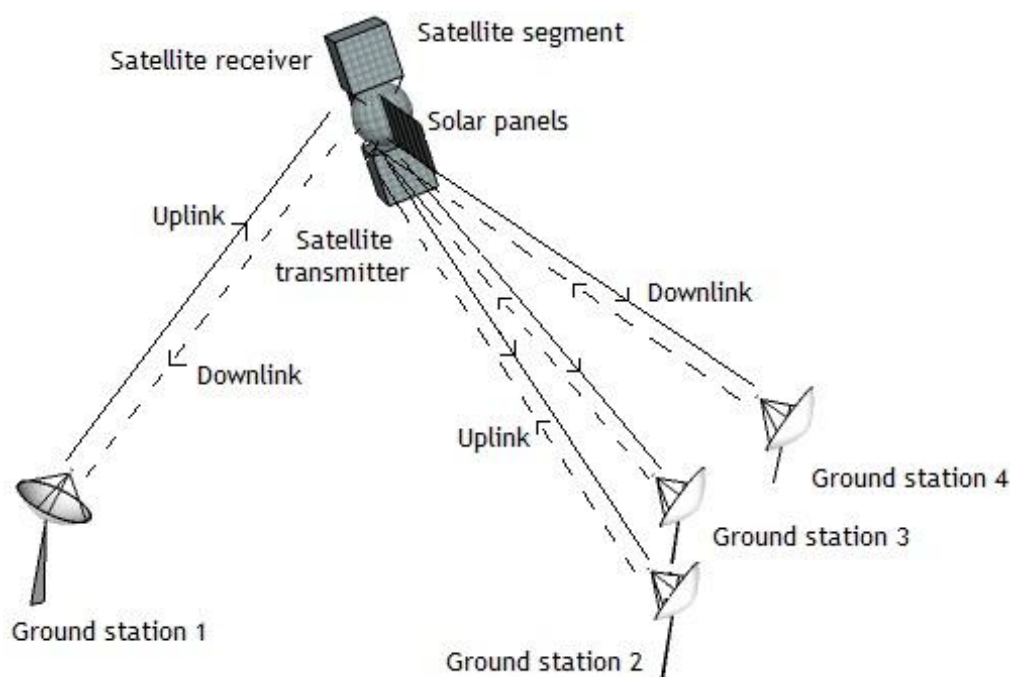


Figure 2.24 - Bi-directional communication between ground segments through a satellite station

There are two types of communication satellites:

- Active: It operates as a repeater which amplifies the RF signals obtained from Earth stations, retransmitting them then. However, those retransmitted signals will not have the same power as the ones received.
- Passive: It acts as a mirror, only reflecting the RF signals to ground stations. Nowadays, they are rarely used comparing to active communication satellites.

Concerning to that, the active satellites will be used for the tracking of satellites in this thesis.

2.8.1 Satellite Orbits

Satellite orbits can be ordered in two main groups: Non-geostationary Earth orbit (NGSO), and Geostationary Earth Orbit (GSO).

A NGSO is characterised for being a low Earth orbit, where its orbital heights (altitudes) are not located far away from the Earth. Subsequently, the altitudes of those satellites are lower than 10000 km; exploring that, there are sorts of characteristics which define a NGSO, such as: low transmission delays of data communications; the possibility to cover the highest latitudes with a higher resolution; and the associated low cost of satellites orbiting at those altitudes which require low cost antennas operating in VHF or UHF frequency bands. The different types of orbital altitudes are [20, 21]:

- Low Earth Orbit (LEO): Satellites are orbiting at average altitudes of 1000 km in a circular form. The typical range varies from 500 km to 1500 km, consonant the satellite. The orbital period¹¹ varies from 1.5 hours to 2 hours.
- Medium Earth Orbit (MEO): Satellites are orbiting at a typical altitude of 10400 km in a circular form. Although, the rotation varies from 5000 km to 25000 km, consonant the satellite. The orbital period is of approximately 6 hours.
- Highly Elliptical Orbit (HEO): The orbit is characterised to be elliptical, mainly appropriated to communicate with high latitude Earth places. They are described by its apogee and perigee, which define the maximum altitude and the minimum altitude of a satellite orbit. Usually, Molniya orbit is referred to be a notable case of HEO; its apogee lies over a 39000 km altitude and the perigee is located at an altitude of 1000 km. The orbital period is of approximately 12 hours.
- Geosynchronous Orbit (GEO): Satellites are orbiting at an average altitude of 35786 km in an equatorial circular form. The orbital period is of approximately 23 hours and 56 minutes. The longitude is the only parameter that varies along the movement, once latitude remains the same.

Figure 2.25 shows the orbit of the different orbital altitude types. MEO is not shown though, due to the similarities with LEO in terms of circular orbital shape. Beyond orbital heights, non-geostationary Earth orbits are defined by the inclination of the orbital plane compared to the equatorial plane, which is the centred Earth's angle by default. The angle is evaluated from 0 degrees to 180 degrees. Thus, the different angle configurations are called as:

- Equatorial orbit: it is defined by the superposition of both equatorial and orbital planes, which outline inclinations of about 0 degrees.
- Polar orbit: demotes inclination angles of about 90 degrees, with a pole-to-pole rotation.

¹¹ Orbital period is the time that a satellite takes to make one complete rotation around Earth's axis.

- Inclination orbit: refers to the rest of the possible angle configurations.

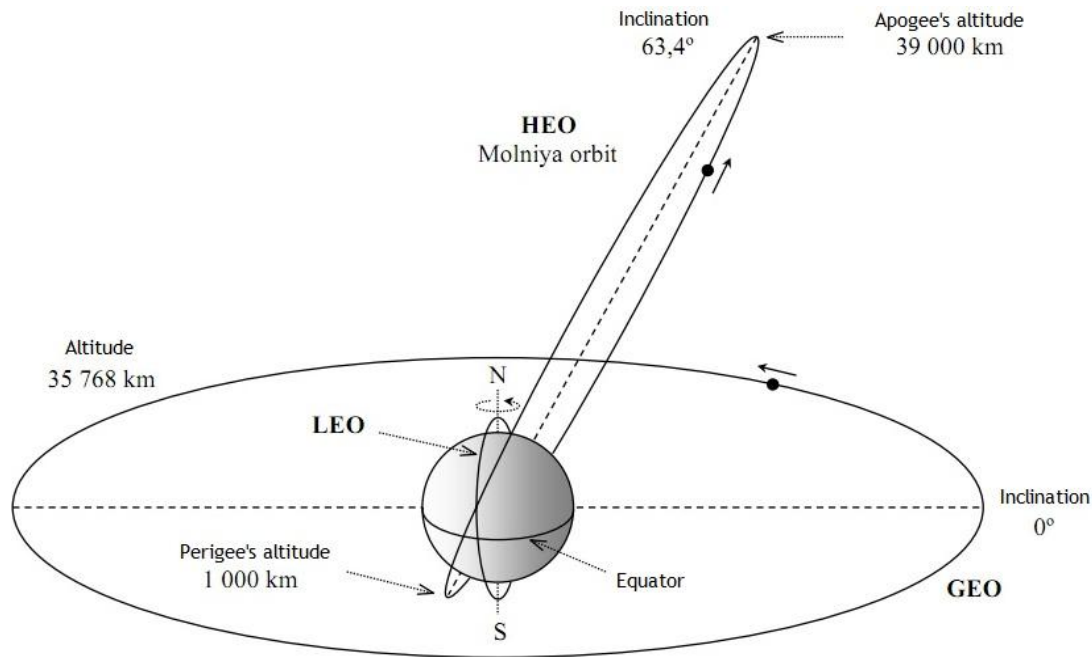


Figure 2.25 - Orbital altitudes of satellites (adapted from [20])

A GSO works similarly to GEO. As a result, satellites at geostationary Earth orbit are positioned at a fixed altitude with a constant radius of 35786 km, rotating around the equatorial plane of the Earth; then, any point on earth will be unchanged relatively to GSO satellites.

Next, the comparison of satellite orbits is presented in in Table 2.3.

Table 2.3 - Different orbit properties [20]

	LEO	MEO	HEO	GEO
Earth's coverage	Large-scale	Large-scale	1/2 to 1/3	1/2 to 1/3 (Poles not covered)
Tracking of satellites	Needed	Needed	Not needed	Not needed
Required constellation	≥ 48 satellites	≥ 10 satellites	3 satellites	Not needed
Losses	Small	Medium	High	High
Delay	5-7 ms to 10-25 ms	70-100 ms	150-300 ms	250 ms

Analysing Table 2.3, the usage of LEO is more adequate for the tracking of satellites purpose in this thesis; that is why it will be the most focused orbit.

The different types of orbits, or the time varying of a satellite in an orbit, require different proceedings for the tracking of satellites by a parabolic antenna. That is, a

coordinate system which reflects the modification of a satellite orbit must be defined as a function of the following three coordinates of visibility:

- Azimuth (β): The angle of rotation around a vertical axis; it is measured from the geographic North (0° by convention) towards the point where the satellite seems to be when observed from Earth along its horizon, in a clockwise sense. The measurement is effectuated in degrees, and it varies from 0 degrees to 360 degrees.
- Elevation (α): The angle that the dish of a parabolic antenna does above Earth's horizon when pointing to a satellite. The measurement is done towards the sky and it varies from 0 degrees to 90 degrees.
- Distance (d): The straight line distance from the parabolic antenna of a ground station to the satellite. Usually, it is measured in km.

Thus, a parabolic antenna must aim at the sky in order to find a satellite, taking into account the referred azimuth and elevation coordinates. The distance is only important to evaluate the type of orbit. As an example, GEO satellites are always visible from the ground station, when positioned in an enclosed region. Figure 2.26 describes the respective coordinates. The circular polarisation plays an important role, because is related with the relative movement of satellites and consequently its altitude changes.

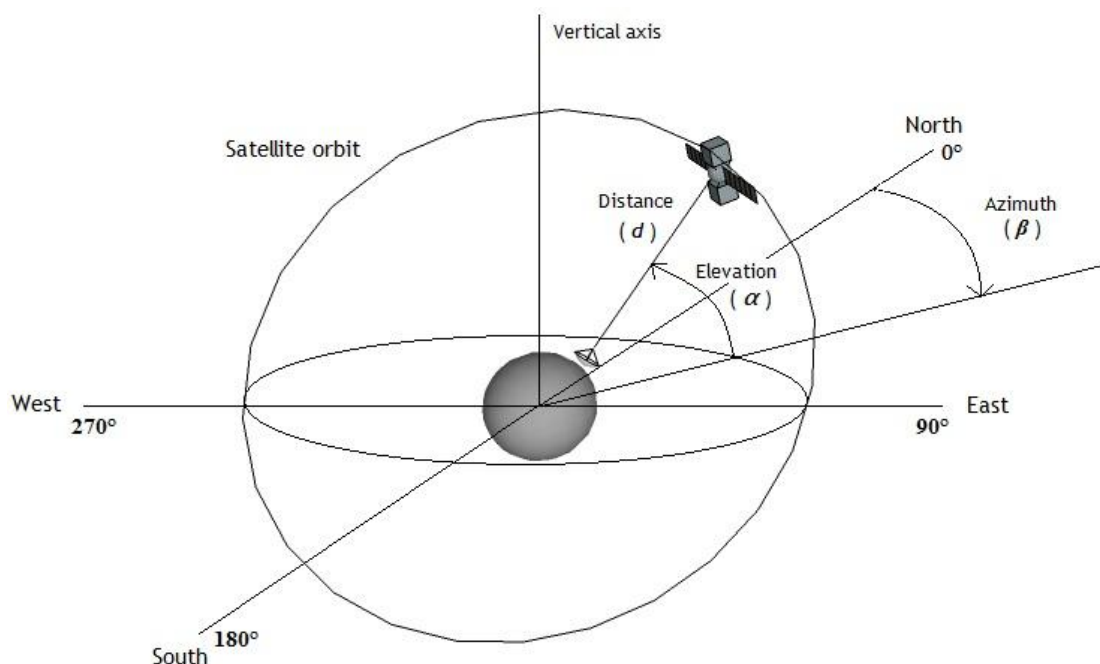


Figure 2.26 - Coordinate system describing a ground station-satellite communication

Chapter 3

Work Description

This chapter contains a presentation of the work developed in this thesis. First, an explanation concerning the choice of the planar equiangular spiral antenna (PESA) is given, taking into account its advantages to the others. After that, all the implementation of PESA as a feed will be described in three steps.

3.1 The Choice of Planar Equiangular Spiral Antenna

Planar equiangular spiral antennas reveal a set of qualities that distinguish them from the rest of the analysed antennas. Firstly, the main benefit of PESA is its potential to emit in a circular polarisation (see section 2.3.8). This is a very important parameter that distinguishes a broadband antenna from a narrowband antenna. At very high frequencies the polarisation becomes elliptically, reflecting its good efficiency through a wide bandwidth range. Also, the directivity (see section 2.3.3) is illustrated by a single beam that irradiates onto the dish; thus expressing its high concentration of power through a direction. Note that this is very important, because a reflector (parabolic) antenna needs a high directivity to establish connection with a satellite. The radiation pattern (see section 2.3.1) of such an antenna will radiate perpendicularly to its plane, which is a wished aspect again. In a parallel way, bi-directional radiation will be provided, thus the use of a ground plane to reflect the RF waves is a mostly wanted effect. VSWR (see section 2.3.7) is rarely higher than two for the intended bandwidth, especially when the frequency is augmented; hence enabling a matching with the transmission line. Note that longer spiral arms tend to be more efficient while radiating. Finally, as a finite structure, PESA exhibits the characteristics of an infinite structure.

3.2 The implementation of the feed

The implementation of PESA was made in two steps:

- Design;
- Fabrication;

At the design part, a printed circuit board (PCB) was designed as a platform for the antenna itself; then, its printing on the PCB corresponds to the first part of the fabrication process. Subsequently, the next part was the soldering of a coaxial cable to feed the spiral arms of the antenna.

The two stages of implementation are described ahead.

3.2.1 Design

The design of the antenna PCB to install on the parabolic antenna involved the usage of two software programs:

- *MATLAB* [22]
- *Ansoft HFSS (version 13)* [23]

In a first stage, the use of *MATLAB* software was crucial to create the initial outline geometry of PESA. A sketch of the script developed (see Appendix A) to represent the shape of the antenna is shown in Figure 3.1. Note that the parameters $a = 0.35$ and $K = 0.597$ were chosen in order to follow [16]. For more information about them see section 2.7

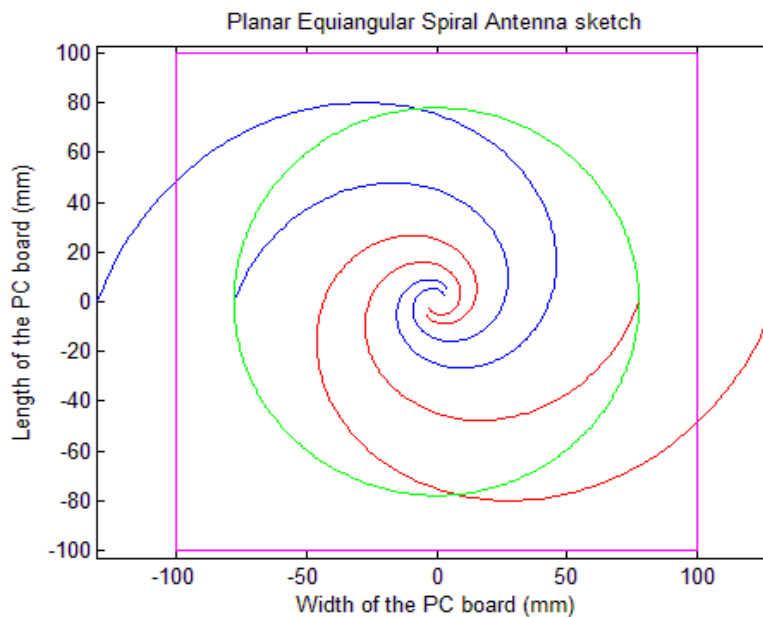


Figure 3.1 - PESA plot in *MATLAB*

Analysing the plot, one verifies that the two red spirals (curves) describe one arm, as well as the two blue spirals (curves) describe the other arm of the antenna. Although, the spiral arms must be finite; hence a green circle was plotted to allow that. The blue and red curves outside of the green circle do not belong to the final design of the spiral; this means that the points that intersect the green circle (see Figure 3.2) are those which define the outer limits of the arms. Note that the purple square measures the dimensions of the printed circuit board (PCB), which was scaled as 200 mm \times 200 mm.

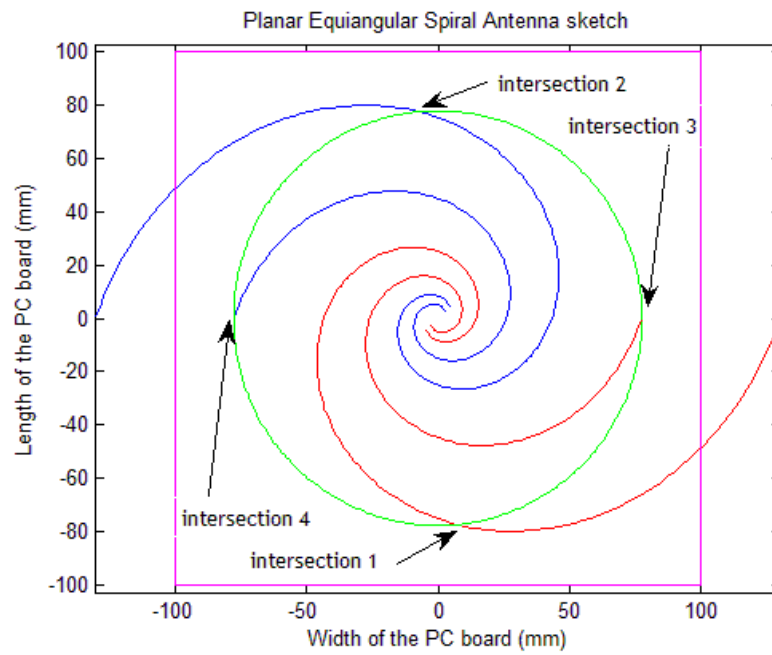


Figure 3.2 - The intersection points in order to create finite arms

At last, the desired final shape of the antenna is represented in Figure 3.3 - in this case the model has LHCP.

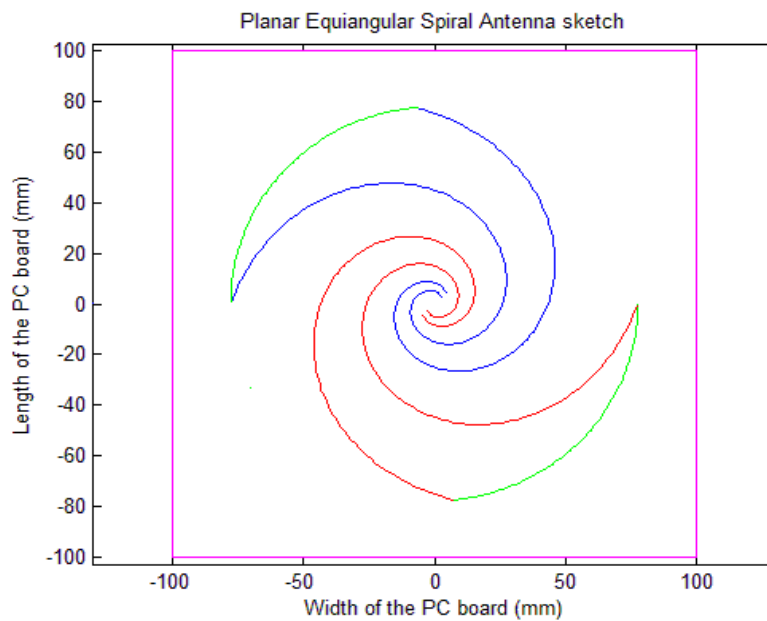


Figure 3.3 - The desired final shape of PESA

Once the first part of the design got completed, *Ansoft HFSS* came on a second part in order to simulate some of PESA parameters. The complete design of PESA is represented in Figure 3.4.



Figure 3.4 - PESA model in *Ansoft HFSS* as a whole: front and back sides of the designed PCB

For the front part of PESA, the green layer of the model is the substrate (with a very thin thickness) held along PCB. The orange layer is made of copper - in order to enable the electrical conduction. One can also see that the two arms are suspended in free space; therefore, they are also part of the substrate. Actually, that means they will work as two spiral slots (see section 2.7). The model was also modified at the terminals region, allowing the balanced feeding of PESA structure; also, a lumped port was added at the same origin, to excite the movement of electrons (to generate current). This is required for the measurement of S-parameters. A close-up of the lumped port at the terminals of the antenna is shown in Figure 3.5.

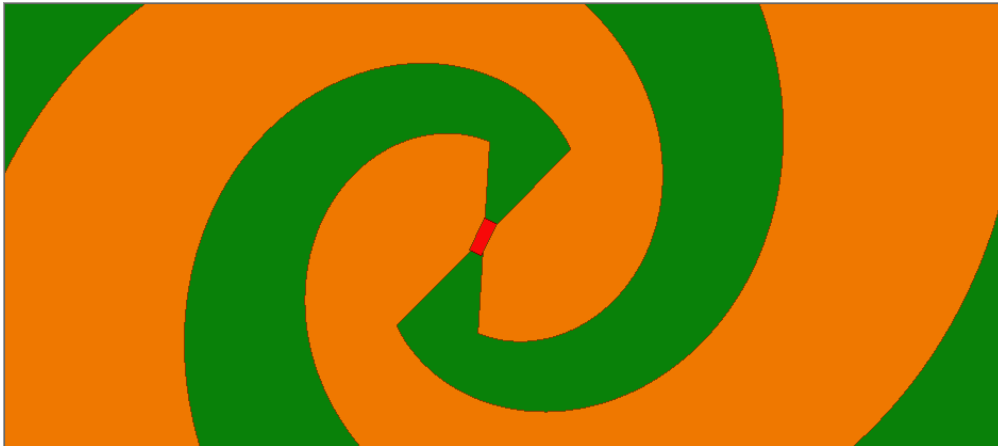


Figure 3.5 - A close-up of lumped port (red color) at the origin

Meanwhile, in order to enable a real simulation, an inclusion of a BNC RF connector (see Figure 3.9) is required to substitute the coaxial cable used for the practical antenna (see section 2.7.1). That BNC RF connector model was also used to feed the antenna. Then, two cylinders were drawn; one being the inner conductor with a radius r_{inner} of 0.65mm, and the outer cylinder with a radius:

$$r_{outer} = r_{inner} * e^{-\left(\frac{5}{6} \times \sqrt{\epsilon_{ps}}\right)}$$

Where:

r_{outer} - Radius of the outer cylindre made of Teflon;

r_{inner} - Radius of the inner cylindre made of copper;

ϵ_{ps} - Relative permittivity of the isolation material of BNC RF connector; Teflon (≈ 2.1) in this case.

At one end the inner conductor reached out the structure to feed, and at the other a full solid copper cylinder of the same radius as r_{outer} was applied. In the end, the whole connector had 70mm long. Figure 3.6 shows the procedure.

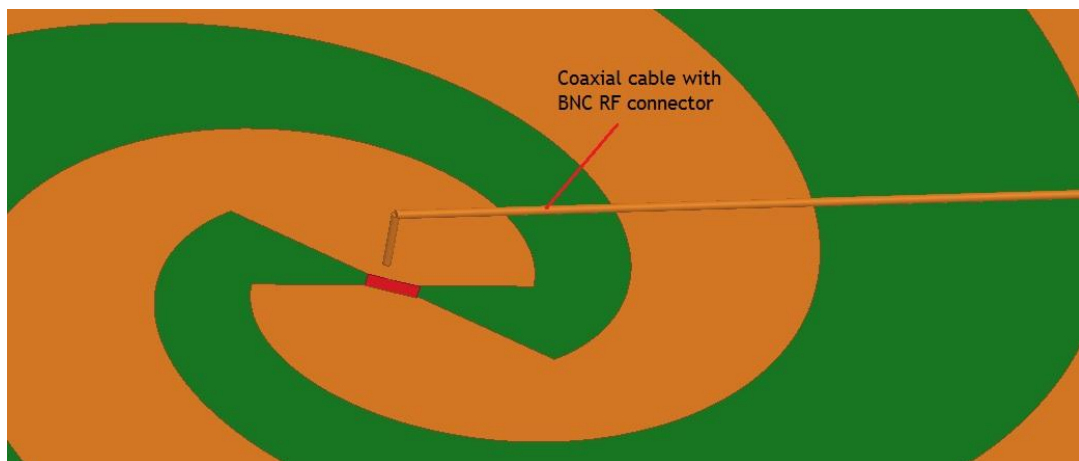


Figure 3.6 - A close-up of BNC RF connector

Finally, an air box was drawn to permit infinitely radiation of the waves far away from the source; that is, a far field was created. Note that the simulation was also made with a reflector acting as a mirror, because PESA is able to radiate in bi-directionally; although only one way radiation is wanted, in order to concentrate more energy. Figure 3.7 shows both configurations of PESA with an air box.

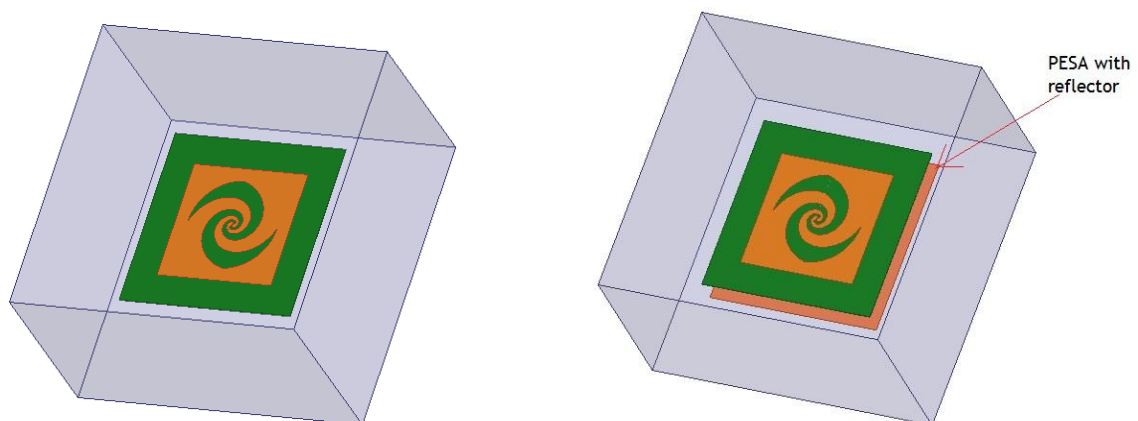


Figure 3.7 - The PCB inside an air box - with a reflector on the right

The simulation of its parameters will be discussed in Chapter 4Chapter 4.

3.2.2 Fabrication

After the design of PESA, the manufacturing process of its PCB took place. Consequently, the model of Figure 3.4 was converted into a physical PCB, where the process of photolithography is the key. Therefore, the respective *hfss* extension was converted and exported as an extension called *IGES* which is accepted by *Advanced design System 2009 (ADS)* [24] . The latter generated the required *Gerber* extension with a high resolution, and was printed onto a transparency with the final dimensions of PESA PCB. Finally, the fabrication of the physical PCB was made by photolithography¹², which consisted on the following procedure:

- The photomask that was generated and revealed from the Gerber extension was printed by a laser printer and exposed when mixed with a chemical solution.
- Some parts of the photoresist¹³ contained on the PCB - in this case a FR4 model - were exposed to UV light (a black light). While this process was running, the photomask which contained the model of PESA was placed over the PCB, in order to print the model on the exposed photoresist by hardening it.
- After that, the exposed photoresist was cleaned and the copper was revealed.
- Then, the PCB was dipped into a chloride solution to etch the copper formed around the arms of the spiral.
- Finally, the PCB was cleaned with running water.

As a result, the final PCB was created. Its representation is shown in Figure 3.8.

¹² Photolithography is a process which uses light to transfer a geometric shape of a photomask (acetate sheets with a circuit board model) onto a surface.

¹³ A photoresist is a chemical material that is sensitive to the light allowing the formation of pattern shapes on a PCB surface. It consists on the top layer of the PCB.



Figure 3.8 - The PCB of PESA - left part represents the top and right part represents the bottom

In order to feed PESA, a RG-174/U coaxial cable with an impedance of 50 ohm connected to a BNC RF connector¹⁴ (also of 50 ohm) was used. The cable was mounted in a spiral slot form, and soldered onto the copper as described in [16] (see Figure 3.9). The terminals at the origin were soldered to the copper though, as it will be explained ahead.



Figure 3.9 - The PCB of PESA fed by a coaxial cable RG-174/U connected to a BNC RF connector

¹⁴ BNC (Bayonet Neill Concelman) connectors are coupled to coaxial cables to enable their connection with radio frequency instruments, acting as a RF connector. It is suitable for frequencies under 3 GHz.

The method of feed used was the so-called ‘infinite balun’ method (see section 2.7.1), which permits a balanced way of feeding the balanced structure. Firstly, one cable was fixed with an approximate distance to both edges of a copper arm, in order to take advantage of the conduction. Hence, this cable works as an outer conductor which feeds PESA from the outside. Then, in order to keep the symmetry of the structure and to avoid disturbances in the radiation pattern, a dummy cable (also a RG-174/U cable) was also mounted on the other arm (this cable is shorter though). Now, looking at the origin with more detail (Figure 3.10), one can see the copper core of each cable was exposed, in order to establish the physical connection between the antenna and the cable. Therefore, the feed cable was soldered to the terminal of the other copper arm, where the dummy cable was mounted; the dummy cable copper core was soldered to the same terminal. Note that the copper mesh of each cable was also soldered to the respective terminals. A reflector was also built (Figure 3.11) in order to establish a one way radiation, as described in 3.2.1 . Finally, the fabrication of the antenna was completed, and now the balanced PESA is concluded.

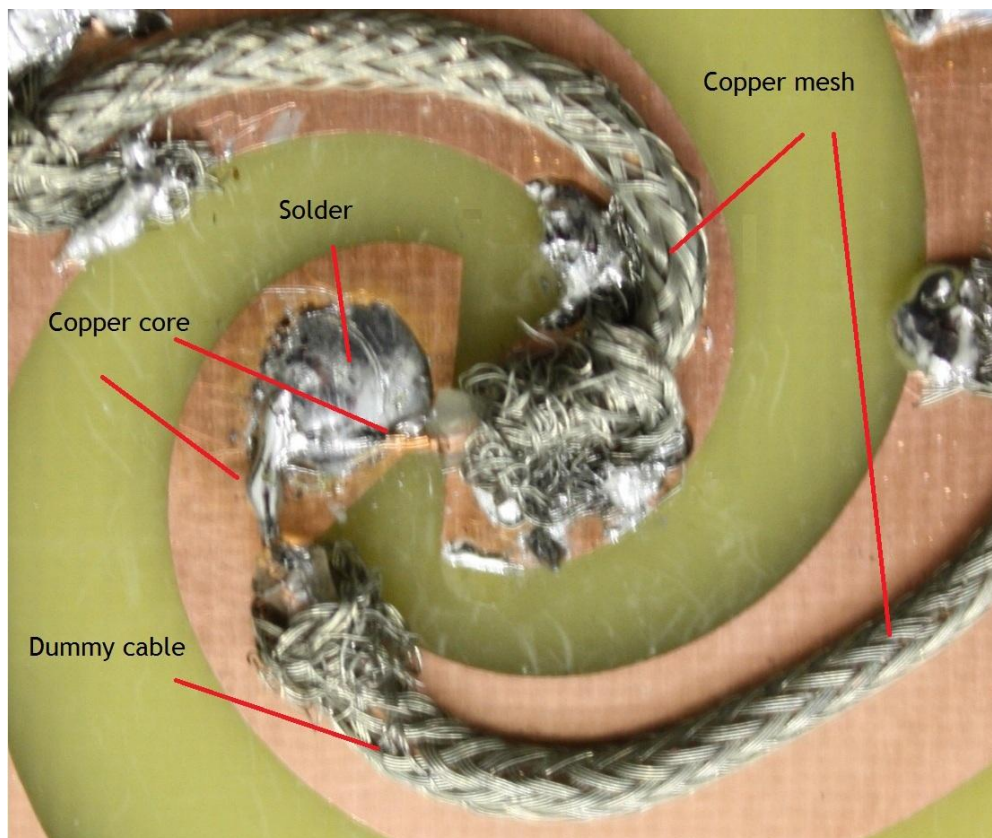


Figure 3.10 - Feeding of PESA structure in detail



Figure 3.11 - Metallic reflector

Chapter 4

Software Simulation

In this chapter, the simulation results of PESA design made in *Ansoft HFSS version 13* (see 3.2.1) are presented. Some of antenna parameters (see section 2.3), such as radiation pattern, gain, directivity, HPBW, voltage standing wave ratio, and return loss were tested. Note that the simulations of return loss and VSWR were made for the case of PESA radiating in a bi-directional way, and for the case of PESA radiating only one way with a help of a reflector as wished (see Figure 3.7), in order to illustrate the differences between both. All the other simulations were made taking into account only a reflector, except for 1.5 GHz while measuring the radiation pattern; again to illustrate the differences between both.

4.1 Return Loss

The simulation of return loss is presented next, for the cases of PESA with and without reflector. Firstly, PESA without reflector is shown in Figure 4.1; the respective frequencies and values of RL (S_{11} in dB) are given in the Table 4.1.

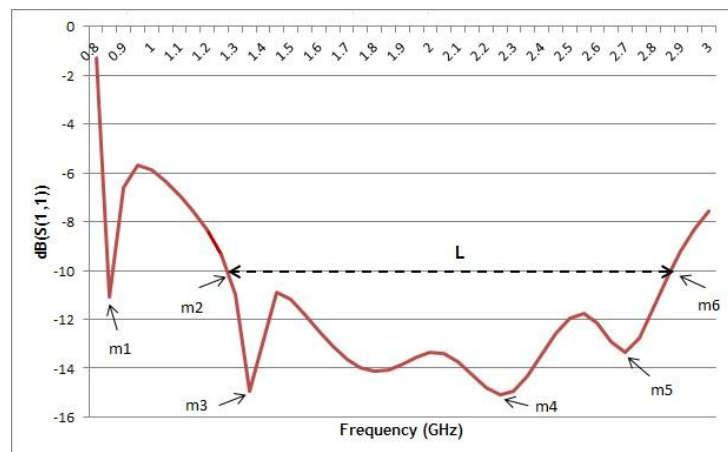


Figure 4.1 - Simulated return loss for PESA without reflector

Table 4.1 - Markers values for figure Figure 4.1

Marker	Frequency (GHz)	S11 (dB)
m1	0.85	-11,0963
m2	1,27	-10
m3	1,35	-15,1109
m4	2,25	-15,111
m5	2,7	-13,363
m6	2,85	-10

As one can see in Figure 5.2, the approximately bandwidth for which the antenna could work as a broadband antenna was between the limits markers m1 and m6 (distance L) of Table 4.1. That is, less power is reflected back to the source and more is delivered to the antenna, when the return loss is below -10 dB for a wide range of frequencies in a spectrum (see section 2.5). Also, the markers m3, m4, and m5 have the best RL results, where there is more power transmitted from the source to the antenna.

The simulation results of PESA with reflector acting as a mirror is plotted in Figure 4.2; the respective frequencies and values of RL (S_{11} in dB) are given in Table 4.2.

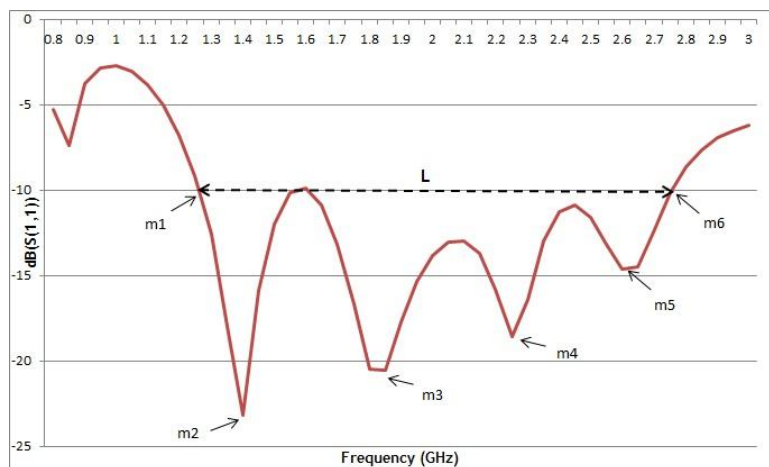


Figure 4.2 - Simulated return loss for PESA with reflector

In this case, as one can see in Figure 4.2, the approximately bandwidth for which the antenna could work as a broadband antenna was between the limits markers m1 and m6 (distance L). Moreover, the markers m3, m4, and m5 have the best RL results, where there is more power transmitted from the source to the antenna.

Table 4.2 - Marker values for Figure 4.2

Marker	Frequency (GHz)	S11 (dB)
m1	1,26	-10
m2	1,4	-23,171
m3	1,85	-20,533
m4	2,25	-18,609
m5	2,65	-14,519
m6	2,75	-10

The comparison between RL of PESA with and without mirror is made in Figure 4.3.

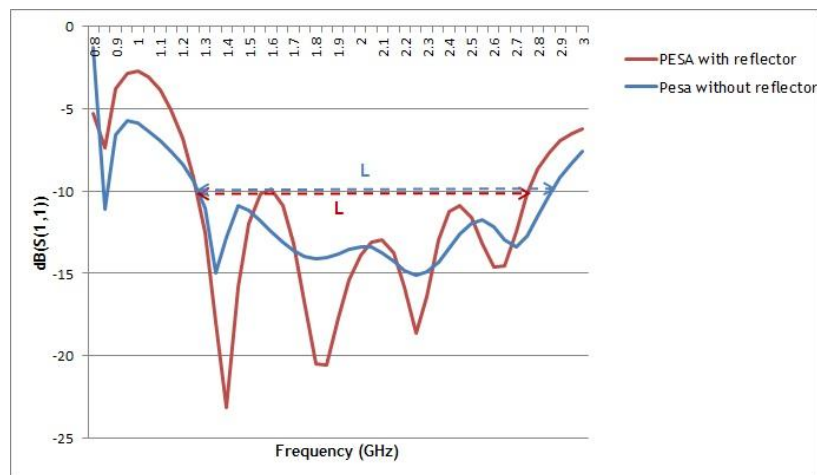


Figure 4.3 - PESA return loss with reflector vs. PESA return loss without reflector

Note that in the important range of frequencies referred for both cases, PESA with reflector took advantage, as one would expect. Therefore, the importance of taking advantage of a reflector is vital; in order to avoid the loss of radiated power in the operating direction.

4.2 Voltage Standing Wave Ratio

After analysing return loss parameter, VSWR parameter was evaluated. Again, the simulation was made for the cases of PESA with and without reflector. Firstly, PESA without reflector is shown in Figure 4.4; the respective frequencies and values of VSWR are given in the Table 4.3. Note that the relationship between input reflection coefficient (S_{11}) and VSWR is implicit.

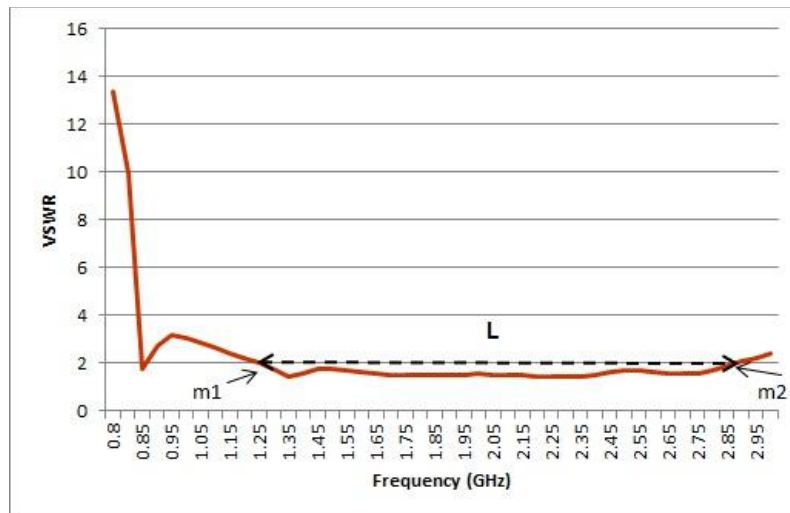


Figure 4.4 - Simulated VSWR for PESA without reflector

Table 4.3 - Marker values for Figure 4.4

Marker	Frequency (GHz)	VSWR
m1	1.27	2
m2	2.85	2

As one can see in Figure 4.4, again the approximately bandwidth for which the antenna could work as a broadband antenna was between the limits markers m1 and m2 (distance L); that is, the range for which the antenna is good matched with the transmission line. As described in section 2.3.7 the matching is good when $1 \leq VSWR \leq 2$.

Now, the simulation result of PESA with reflector acting as a mirror is plotted in Figure 4.5; the respective frequencies and values of VSWR are given in the Table 4.4.

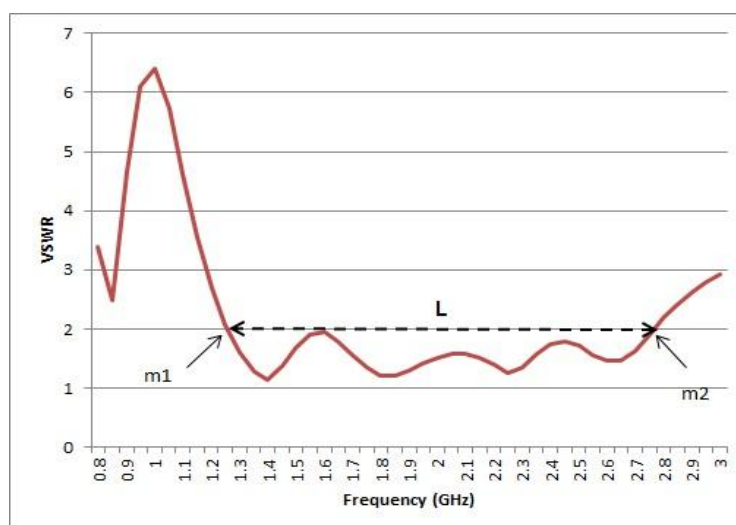


Figure 4.5 - Simulated VSWR for PESA with reflector

Table 4.4 - Marker values for Figure 4.5

Marker	Frequency (GHz)	VSWR
m1	1.26	2
m2	2.75	2

Again in this case, as one can see in Figure 4.5, the approximately bandwidth for which the antenna could work as a broadband antenna was between the limits markers m1 and m2 (distance L).

The comparison between the VSWR of PESA with and without mirror is made in Figure 4.6.

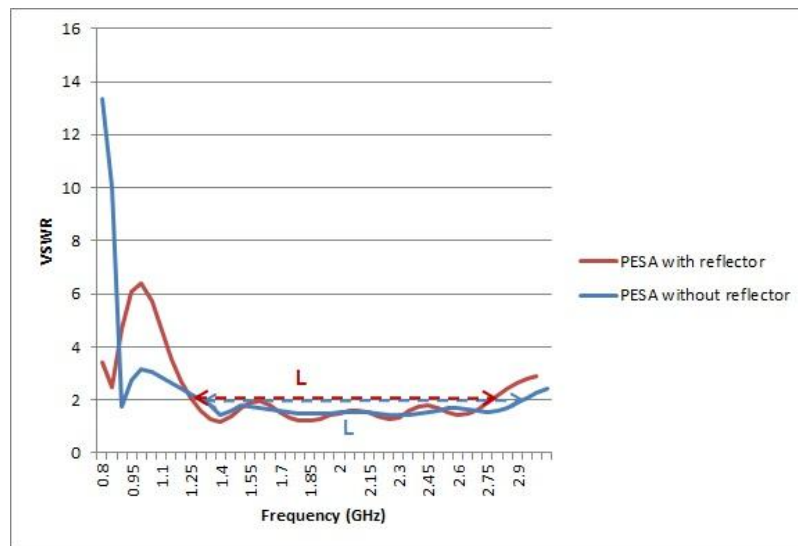


Figure 4.6 - PESA VSWR with reflector vs. PESA VSWR without reflector

Once again, the important range of frequencies referred for both cases, PESA with reflector took advantage, as one would expect. That is, for some values of VSWR, the ones of PESA with reflector are closer to one.

4.3 Radiation Pattern

Radiation pattern has to be measured independently for a desired frequency. In order to follow this requirement, five frequencies were chosen. They are: $f_1 = 1.274$ GHz; $f_2 = 1.5$ GHz; $f_3 = 1.69$ GHz; $f_4 = 2.384$ GHz; and $f_5 = 2.516$ GHz. All those simulated frequencies had good measures of RL and VSWR parameters. Note that, f_1 and f_2 are very close to GPS frequencies L1 and L2 (see section 1.2); thus it is a good reference point. Although, the starting frequency will be f_2 , in order to explain the differences between the radiation pattern of a PESA with a reflector and without a reflector. Note that for each frequency a polar plot and a three-dimensional plot are drawn. Also, note that the radiation pattern components analysed are the E_ϕ and the E_θ patterns; that is, in $\phi = 0^\circ$ and in $\phi = 90^\circ$ plane cuts at different

impedance bandwidth across PESA. The brown curve refers to E_ϕ and the purple curve is refers to E_θ .

4.3.1 Simulation of f_2

The simulated radiation pattern for $f_2 = 1.5$ GHz is given for PESA with reflector and for PESA without reflector. The latter is plotted next in Figure 4.7 and in Figure 4.8, respectively in three-dimensional coordinates and as a polar plot.

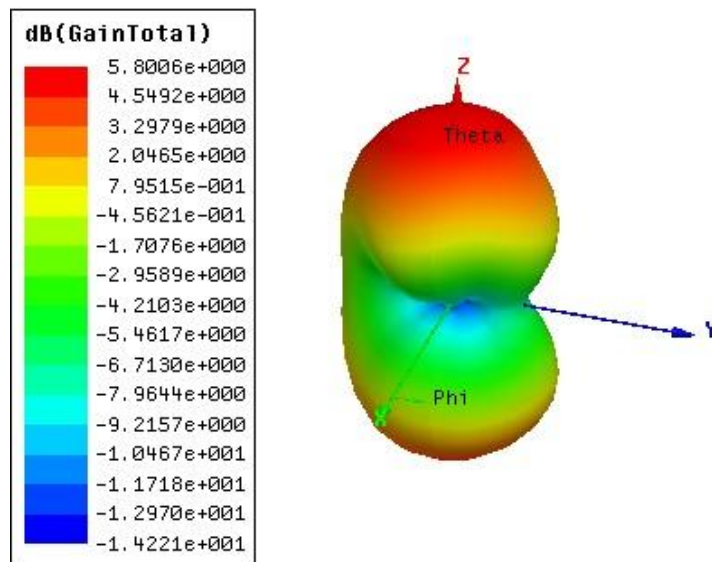


Figure 4.7 - Three-dimensional plot of simulated radiation pattern for $f_2 = 1.5$ GHz (PESA without reflector)

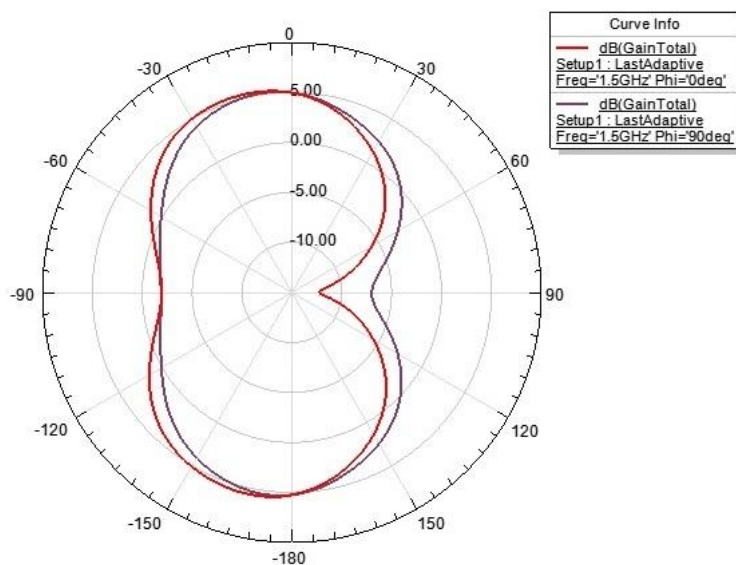


Figure 4.8 - Polar plot of simulated radiation pattern for $f_2 = 1.5$ GHz (PESA without reflector)

Now, the simulated radiation pattern for PESA with reflector is plotted in Figure 4.9 and in Figure 4.10, respectively in three-dimensional coordinates and as a polar plot.

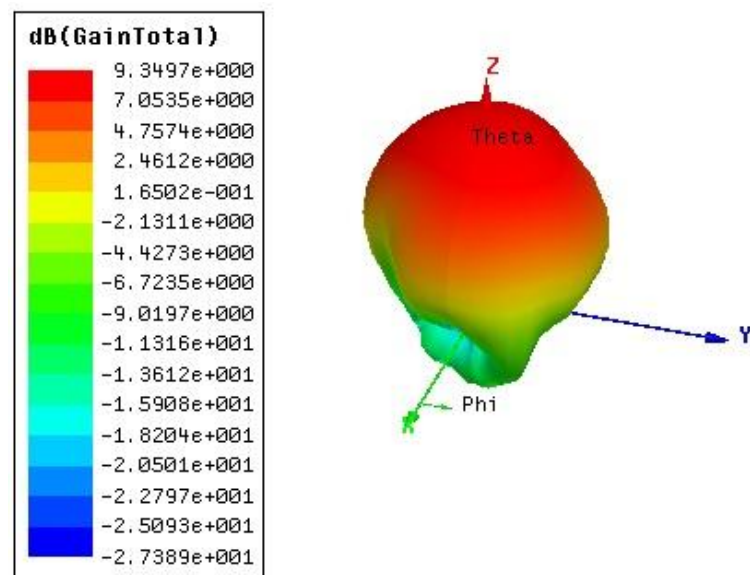


Figure 4.9 - Three-dimensional plot of simulated radiation pattern for $f_2 = 1.5$ GHz (PESA with reflector)

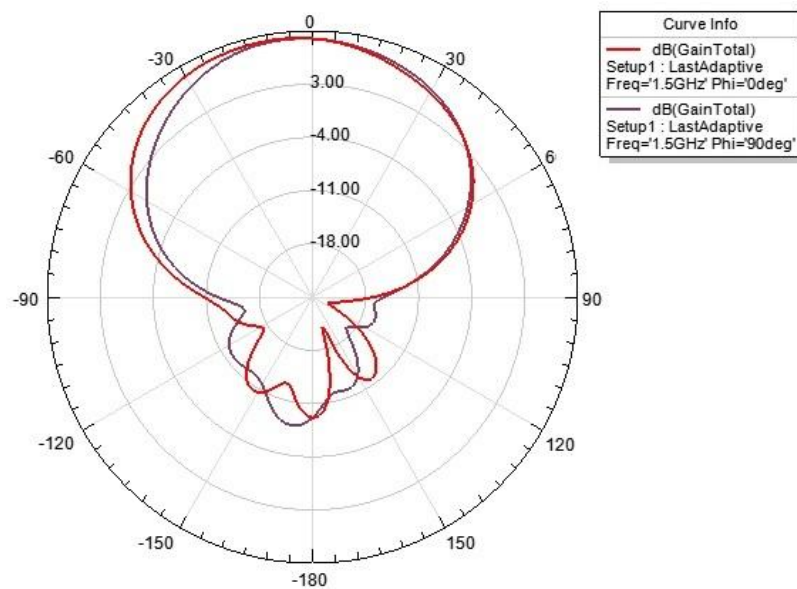


Figure 4.10 - Polar plot of simulated radiation pattern for $f_2 = 1.5$ GHz (PESA with reflector)

Looking at the radiation pattern of each configuration of PESA, one can easily understand the differences in the direction of radiation pattern; that is, for PESA without reflector, the direction of radiation pattern is bi-directional, unlikely for PESA with reflector, as expected. Consequently, the gain for the latter is higher; approximately a bit more than 3 dB of PESA without reflector. Actually, that means two times more when the gain is not in decibels. The

gain of both antennas is represented in Table 4.5. Moreover, HPBW parameter can be calculated, and is represented in Table 4.6.

Table 4.5 - Gain comparison of different PESA configurations for $f_2 = 1.5$ GHz

Structure	Gain (dB)
PESA with reflector	9.3497
PESA without reflector	5.8006

Table 4.6 - HPBW comparison of different PESA configurations for $f_2 = 1.5$ GHz

Structure	HPBW (degrees)
PESA with reflector	69
PESA without reflector	103

Again, one can see that PESA with reflector is more directional (see Table 4.6) and consequently the gain is higher at the direction of main beam radiator (see Table 4.5).

4.3.2 Simulation of f_1

The simulated radiation pattern for $f_1 = 1.274$ GHz is given by Figure 4.11 and Figure 4.12 which show the plot of radiation pattern in three-dimensional coordinates and a polar plot respectively.

Looking at the radiation pattern one can see its unidirectionality (with some back lobes) first. Consequently, the gain is high (about 10 dB). HPBW is equal to 84 degrees.

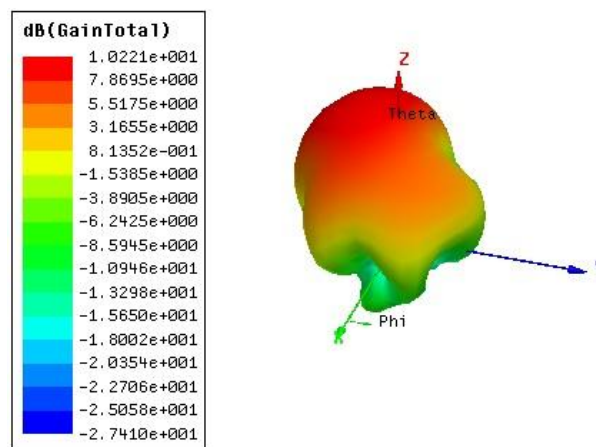


Figure 4.11 - Three-dimensional plot of simulated radiation pattern for $f_1 = 1.274$ GHz

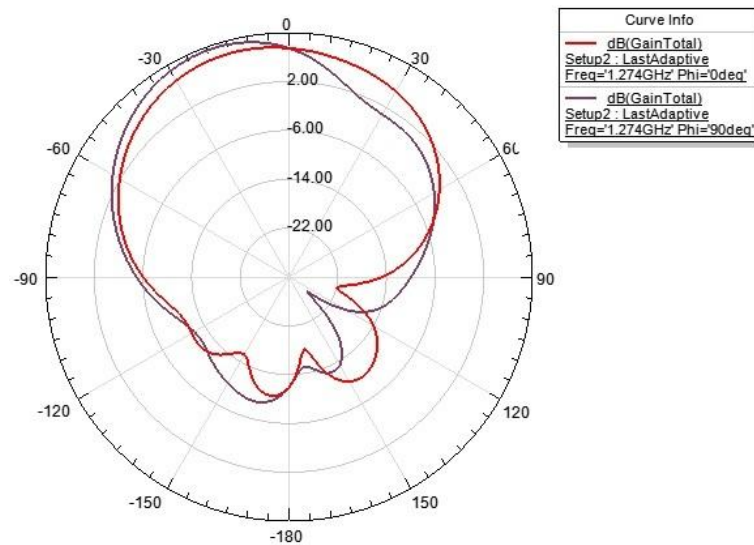


Figure 4.12 - Polar plot of simulated radiation pattern for $f_1 = 1.274$ GHz

4.3.3 Simulation of f_3

The simulated radiation pattern for $f_3 = 1.69$ GHz is given by Figure 4.13 and Figure 4.14 which show the plot of radiation pattern in three-dimensional coordinates and a polar plot respectively.

Looking at the radiation pattern one can see that it is less unidirectional, again with some back lobes. Consequently, the gain is equal to 9.4707 dB. On the other hand, HPBW is equal to 63 degrees.

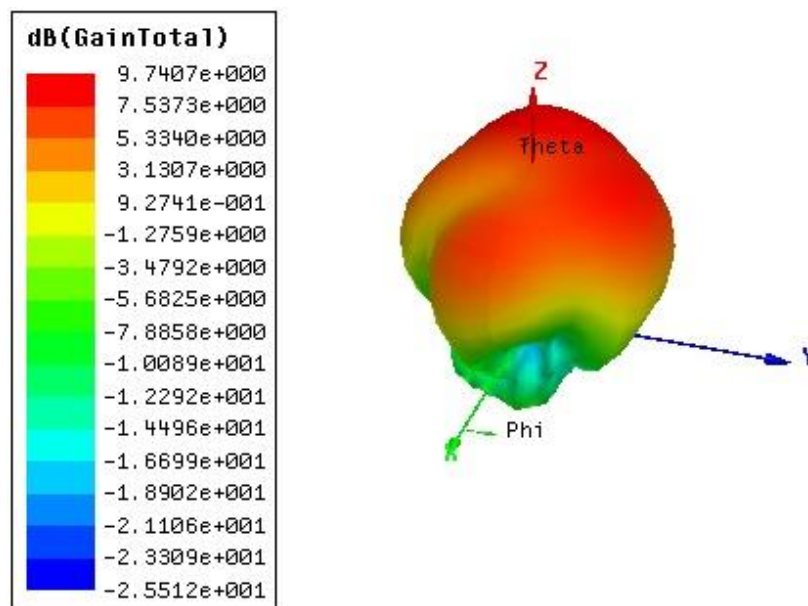


Figure 4.13 - Three-dimensional plot of simulated radiation pattern for $f_3 = 1.69$ GHz

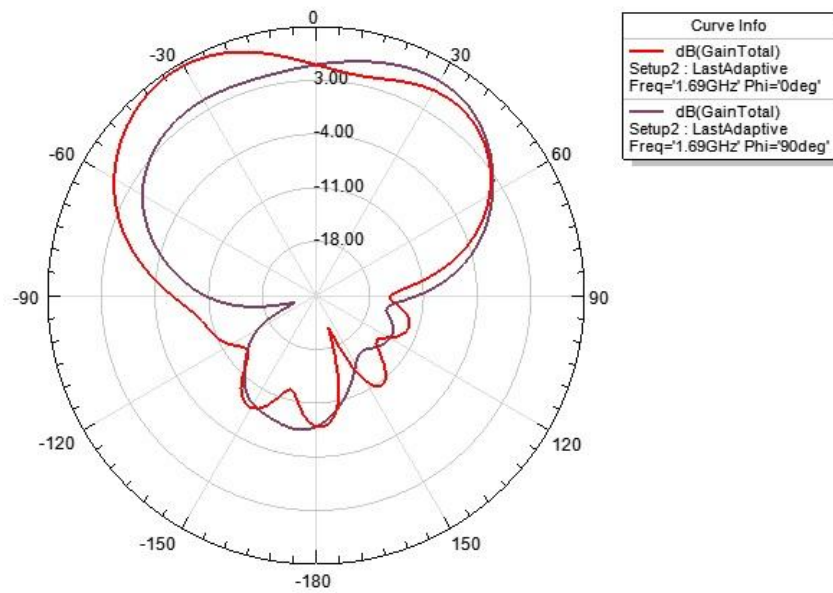


Figure 4.14 - Polar plot of simulated radiation pattern for $f_3 = 1.274$ GHz

4.3.4 Simulation of f_4

The simulated radiation pattern for $f_4 = 2.384$ GHz is given by Figure 4.15 and Figure 4.16 which show the plot of radiation pattern in three-dimensional coordinates and a polar plot respectively.

Looking at the radiation pattern one can see that its unidirectionality has some deviations, again with some back lobes. The gain is equal to 20.6775 dB. On the other hand, HPBW is equal to 61 degrees.

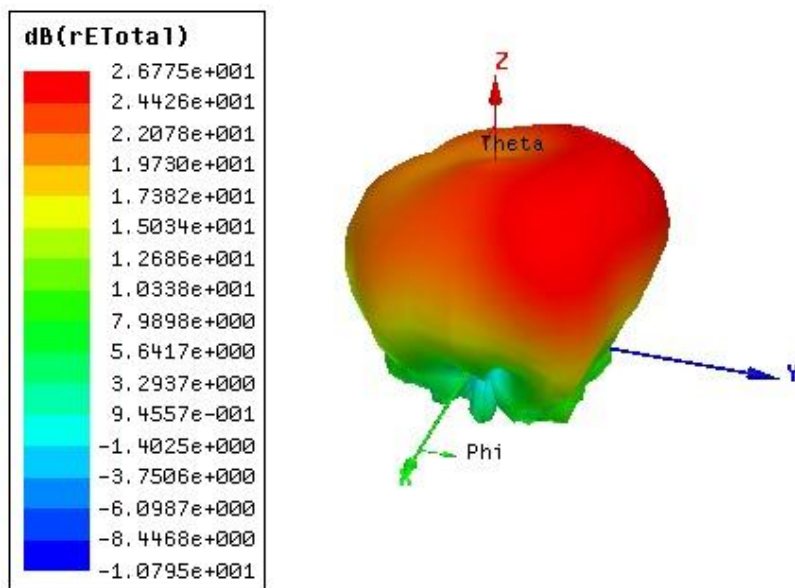


Figure 4.15 - Three-dimensional plot of simulated radiation pattern for $f_4 = 2.384$ GHz

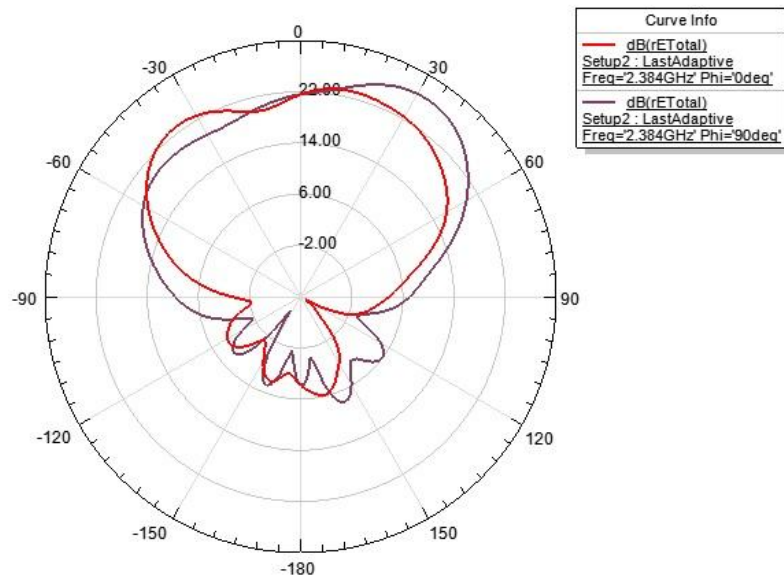


Figure 4.16 - Polar plot of simulated radiation pattern for $f_4 = 2.384$ GHz

4.3.5 Simulation of f_5

Finally, the simulated radiation pattern for $f_5 = 2.516$ GHz is given by Figure 4.17 and Figure 4.18 which show the plot of radiation pattern in three-dimensional coordinates and a polar plot respectively.

Looking at the radiation pattern one can see that its unidirectionality has some deviations (being very wide), again with some back lobes. The gain is equal to 20.6775 dB. On the other hand, HPBW is equal to 52 degrees.

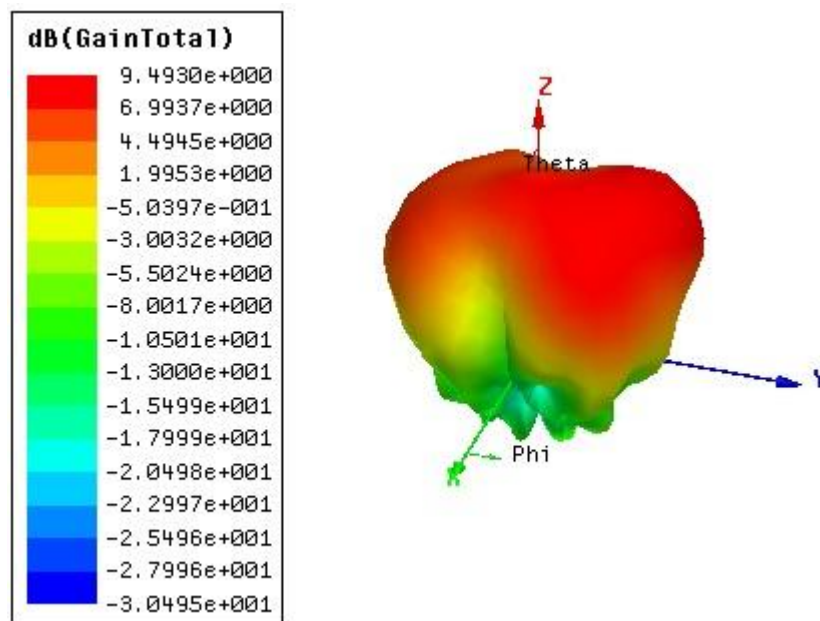


Figure 4.17 - Three-dimensional plot of simulated radiation pattern for $f_5 = 2.516$ GHz

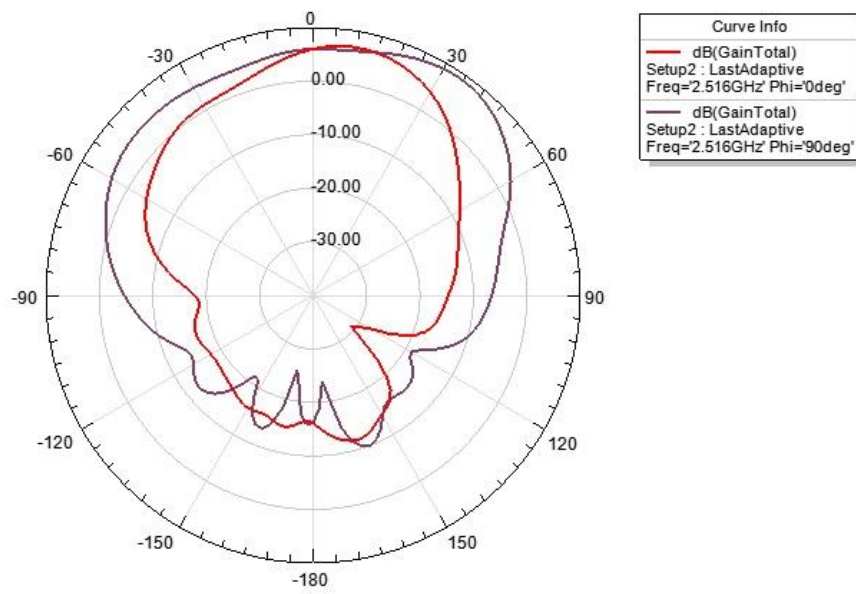


Figure 4.18 - Polar plot of simulated radiation pattern for $f_s = 2.516$ GHz

Chapter 5

Experimental Results

In this chapter the experimental results of the planar equiangular spiral antenna (PESA) designed in Chapter 3 will be presented. The measurements of PESA parameters (see section 2.3) were obtained from the vector network analyser (VNA) of Figure 5.1, and from the anechoic chamber of Figure 5.4 and Figure 5.5. Firstly, a VNA was used to measure S_{11} (in decibels) and VSWR, in order to measure return loss and also the matching between PESA and its transmission line. At the anechoic chamber, the radiation pattern was measured, again with the help of VNA (with the measure of S_{12}). Then, it was possible to evaluate gain, HPBW. Finally, the comparison of experimental results to simulated results (see Chapter 4) is also made.

5.1 Return Loss and Voltage Standing Wave Ratio Measurements

A vector network analyser *Rohde & Schwarz - ZVL model* was the equipment used to measure return loss (RL) and VSWR. The frequency range which the equipment can measure is 9 KHz to 3 GHz; therefore suitable for testing PESA, which lies from 800 MHz to 3 GHz. As all measuring instruments, a VNA needs to be calibrated, in order to minimise measuring errors. Firstly, the calibration used was the so-called full one-port calibration (see Appendix B), which can be applied to each port of VNA; although, in order to measure the parameters RL (see section 2.3.6) and VSWR (see section 2.3.7) the calibration made was only at the input port 1.

Before exposing the measurements, some considerations must be recognised by the reader, in order to establish the connection between the literature review and these practical measurements. Therefore, good results for RL are often referred to be below -10 dB (approximately); this indicates that sufficient power is being delivered to the load (antenna); and subsequently, the more negative RL is, the more power is being delivered to antenna. On the other hand, good results for VSWR mean that for the different frequencies its value should lie approximately between 1 and 2, in order to obtain the required matching between antenna and transmission line. Note that the ideal value for VSWR is 1. Knowing those properties, the measurements of RL and VSWR are presented next.

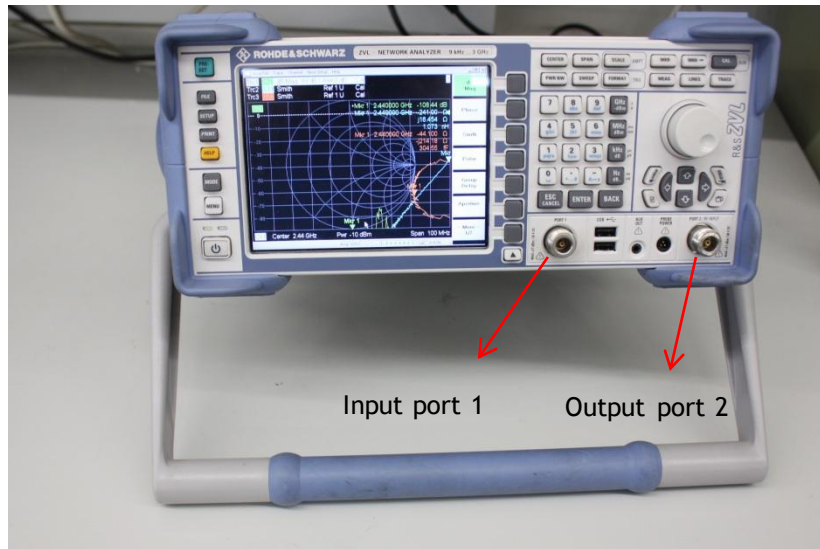


Figure 5.1 - Vector Network Analyser (VNA)

5.1.1 Return Loss

The obtained graphic to return loss was:

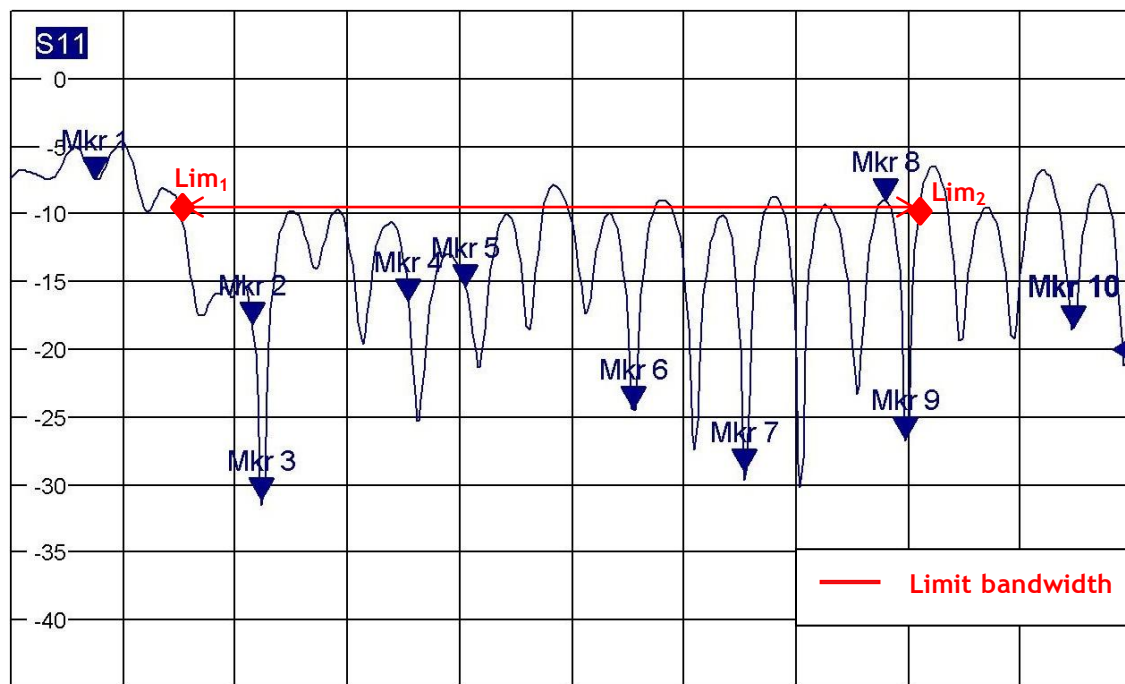


Figure 5.2 - Return loss measurement

As seen in Figure 5.2, the bandwidth for which the antenna works approximately as a broadband antenna (see section 2.5) is between the limits Lim_1 and Lim_2 (regarding to the -10 dB limit); that is, the limit bandwidth. The respective frequencies and values of RL (S_{11} in dB) described in Figure 5.2 are given in the following table.

Table 5.1 - Return loss along several frequencies drawn in Figure 5.2

Marker	Frequency (GHz)	S_{11} (dB)
Mk1	0.970	-6.850
Lim ₁	1.128	-10
Mk2	1.274	-17.909
Mk3	1.292	-28.559
Mk4	1.580	-16.840
Mk5	1.690	-14.875
Mk6	2.020	-25.808
Mk7	2.240	-30.772
Mk8	2.384	-10.120
Mk9	2.556	-27.670
Lim ₂	2.578	-10
Mk10	2.886	-17.147

The markers Mk3, Mk6, Mk7 and Mk9 which were analysed present the best RL values, where there is more power transmitted from the source to the antenna. It is also important to refer that the GPS frequencies (see section 1.2) L1 (1575.42 MHz) and L2 (1227.6 MHz) are under the possibility of being tracked by the parabolic antenna which supports the project.

5.1.2 Voltage Standing Wave Ratio

After analysing return loss parameter, VSWR parameter was evaluated and it comes as Figure 5.3.

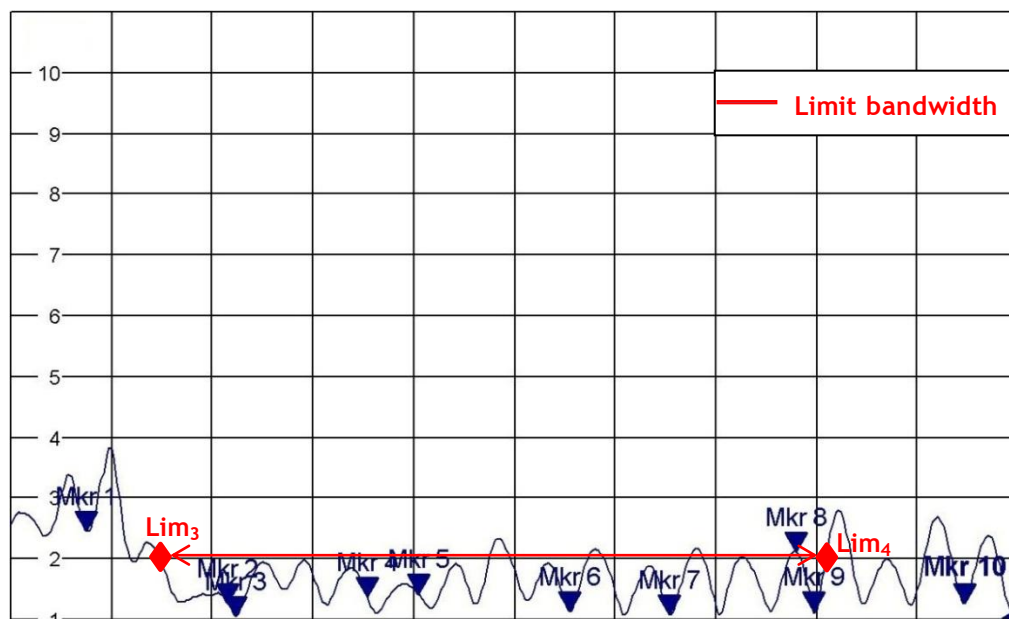


Figure 5.3 - VSWR measured

As one can see in Figure 5.3, the distance between limits Lim_3 and Lim_4 (limit bandwidth) set the range for which the antenna is good matched with the transmission line. Those limits are of course, the same as Lim_1 and Lim_2 , respectively. The respective frequencies and values of VSWR described in Figure 5.3 are given in Table 5.2.

Table 5.2 - VSWR along several frequencies drawn in Figure 5.3

Marker	Frequency (GHz)	VSWR
Mk1	0.970	2.572
Lim_3	1.128	2
Mk2	1.274	1.287
Mk3	1.292	1.069
Mk4	1.580	1.340
Mk5	1.690	1.458
Mk6	2.020	1.144
Mk7	2.240	1.087
Mk8	2.384	1.800
Mk9	2.556	1.124
Lim_4	2.578	2
Mk10	2.886	1.342

Again, markers Mk3, Mk6, Mk7 and Mk9 which were analysed give the best VSWR values, where there is a better matching of transmission line and the tested antenna. That property shows that the relationship between input reflection coefficient (S_{11}) and VSWR is implicit.

5.2 Radiation Pattern measurements

The anechoic chamber at Faculdade de Engenharia da Universidade do Porto (FEUP) was the required place for measuring the radiation pattern of an antenna, and subsequently its gain, and HPBW. It is the ideal place to measure those parameters, because of its special conditions in absorbing EM waves, in order to avoid their reflections. An antenna acting as a transmitter and an antenna under test (AUT) form the essential predicate to obtain radiation pattern measurements. PESA worked as an AUT. Figure 5.4 and Figure 5.5 show the pictures of the basic pillars that provided the measurements at the anechoic chamber.

The VNA of Figure 5.1 was again used in order to measure the scattering parameter S_{21} in decibels (or insertion loss; see section 2.3.6), which allowed the plot of the radiation patterns of some frequencies. Again, the VNA needed to be calibrated in order to receive measures without errors from the transmitting antenna (connected to input port 1) and from AUT (connected to output port 2). Therefore, the calibration used was the so-called one-path two-port calibration (see Appendix B); in order to measure insertion loss (IL), making it possible to plot the radiation pattern of PESA.

In order to compare radiation pattern measurements to radiation pattern simulations, the procedure of section 4.3 is followed once again; that is, five frequencies were chosen:

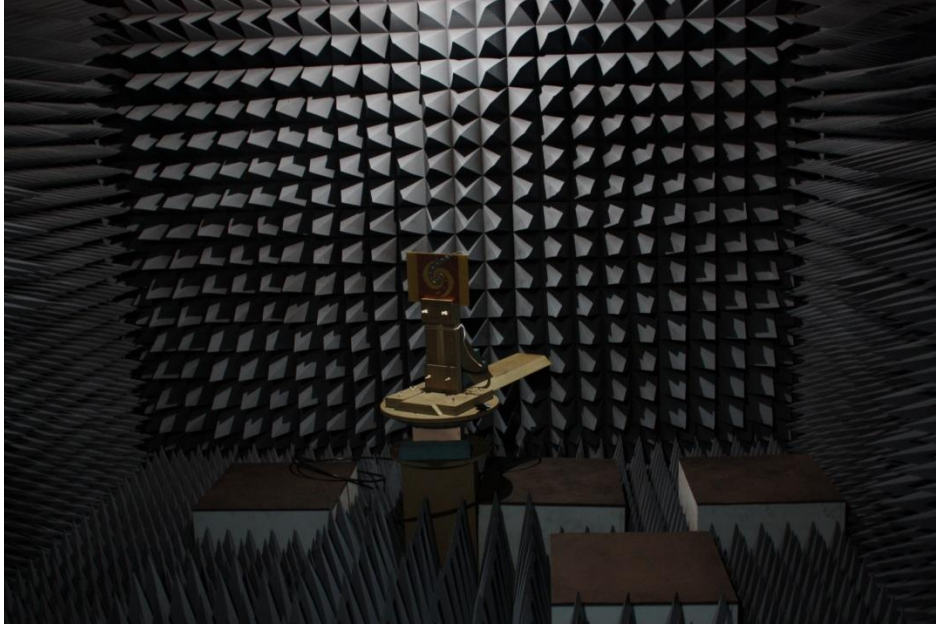


Figure 5.4 - Measurement of PESA (antenna under test) at the anechoic chamber

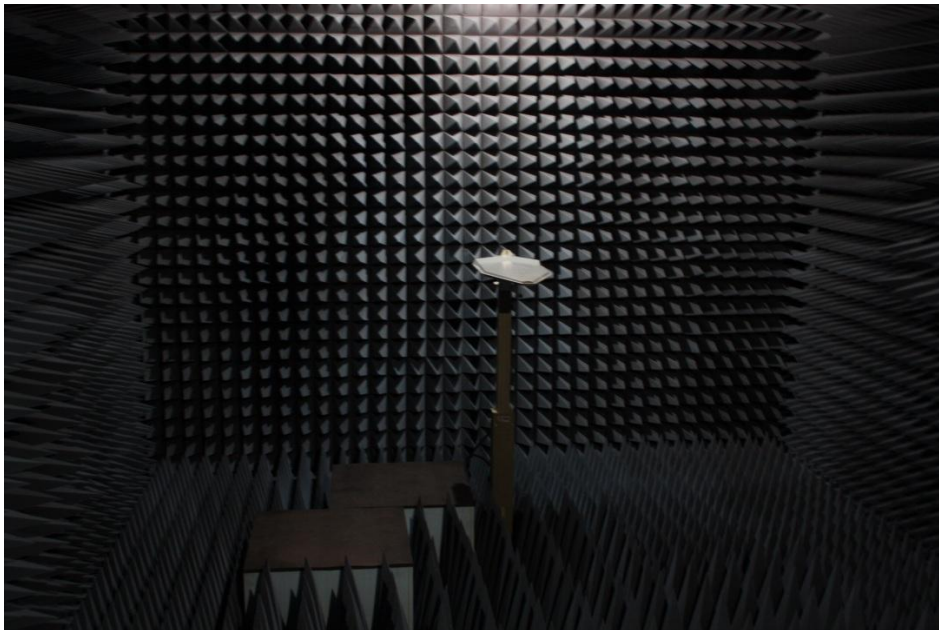


Figure 5.5 - A log-periodic antenna acting as a trasnmmitter (source antenna) at the anechoic chamber

- $f_1 = 1.274$ GHz;
- $f_2 = 1.5$ GHz;
- $f_3 = 1.69$ GHz;
- $f_4 = 2.384$ GHz;
- $f_5 = 2.516$ GHz.

Again, as in simulated results, those frequencies had good measures of RL and VSWR parameters, taking into account the frequencies analysed in section 5.1 . Unlikely simulated

results, the test of the antenna without reflector was not made. Note that for each frequency a polar plot was drawn.

5.2.1 Measurement of f_1

The radiation pattern measured for $f_1 = 1.274$ GHz is plotted in Figure 5.7 as a polar plot of azimuthal plane E_φ , and in Figure 5.8 as a polar plot of elevation plane E_θ (see Figure 2.6). The comparison between both patterns is made in Figure 5.9.

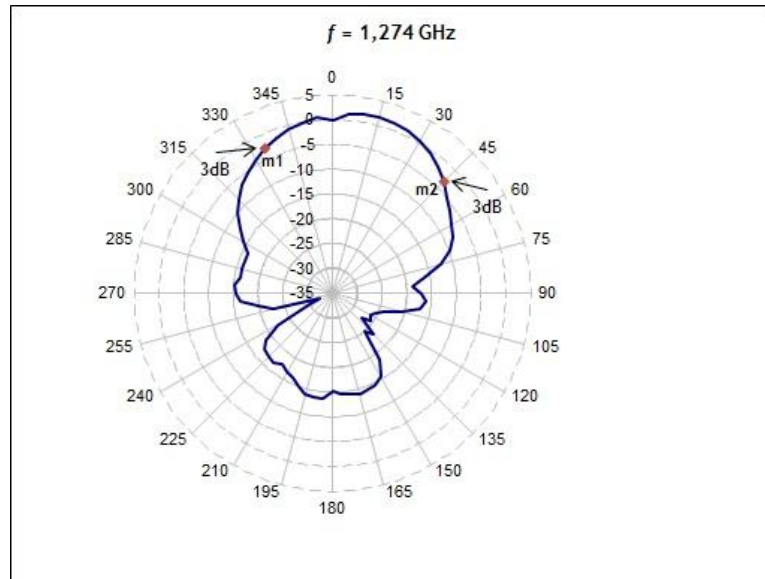


Figure 5.6 - Polar plot of the radiation pattern of E_φ measured for $f_1 = 1.274$ GHz

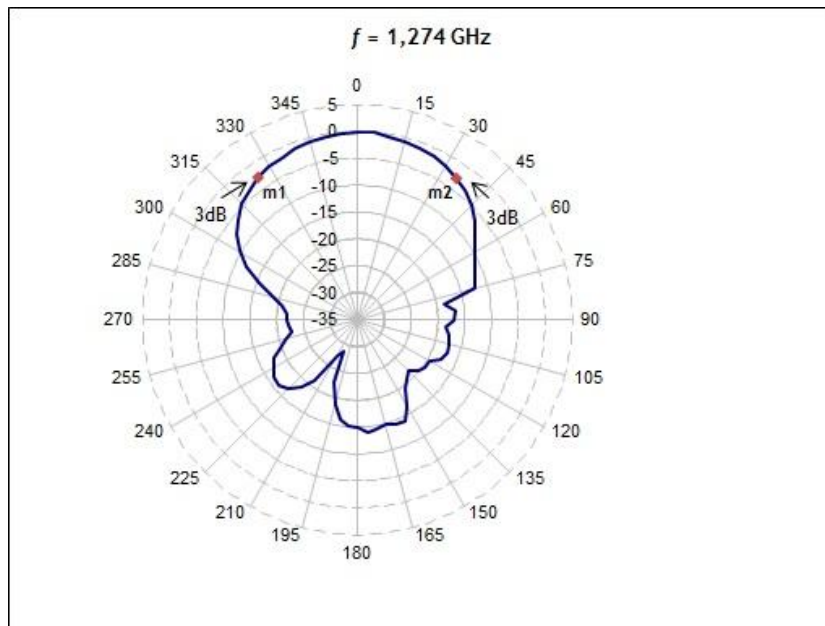


Figure 5.7 - Polar plot of the radiation pattern of E_θ measured for $f_1 = 1.274$ GHz

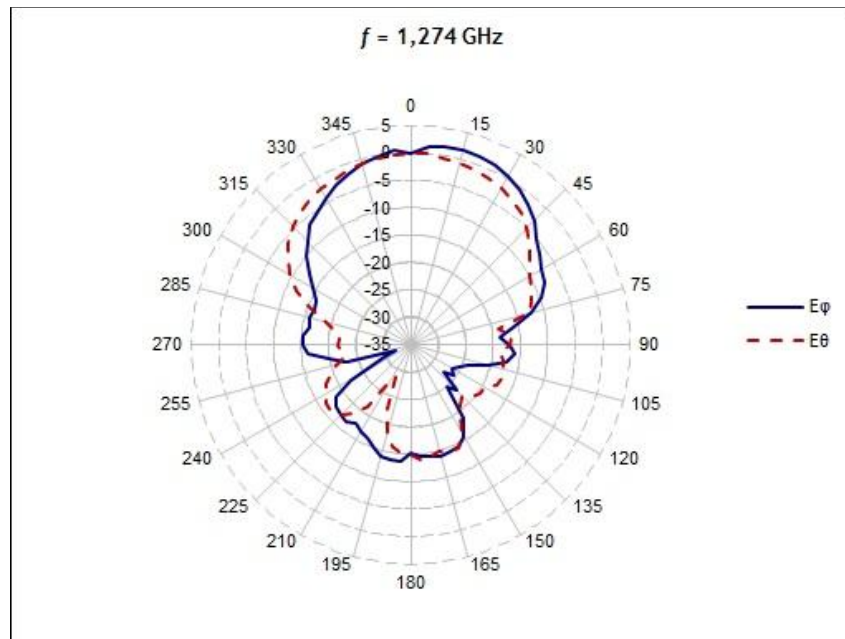


Figure 5.8 - Comparison between polar plots of E_ϕ and E_θ radiation patterns measured for $f_1 = 1.274$ GHz

Looking at the radiation pattern differences one can see that its unidirectionality is present, again with some back lobes. The gain is equal to 1.74 dB in the E_ϕ plane. On the other hand, HPBW is equal to 70 degrees at the same plane.

5.2.2 Measurement of f_2

The radiation pattern measured for $f_2 = 1.58$ GHz is plotted in Figure 5.7Figure 5.9 as a polar plot of E_ϕ , and in Figure 5.10 as a polar plot of E_θ . The comparison between both patterns is made in Figure 5.11.

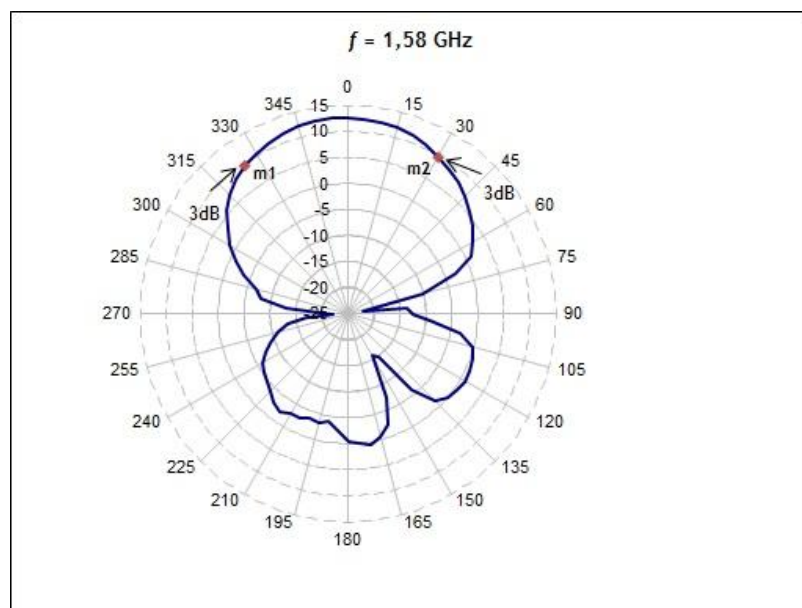


Figure 5.9 - Polar plot of the radiation pattern of E_ϕ measured for $f_2 = 1.58$ GHz

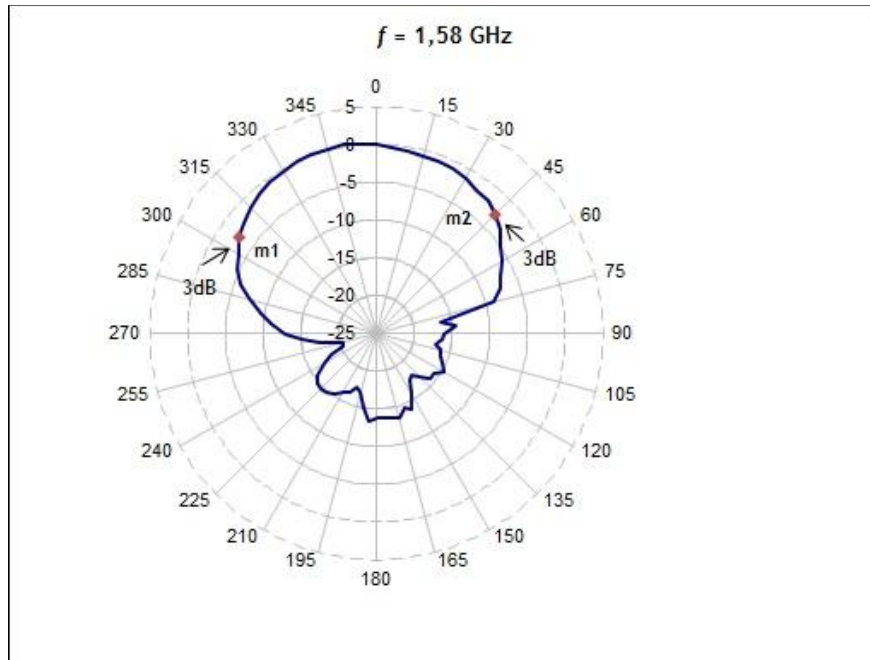


Figure 5.10 - Polar plot of the radiation pattern of E_θ measured for $f_2 = 1.58$ GHz

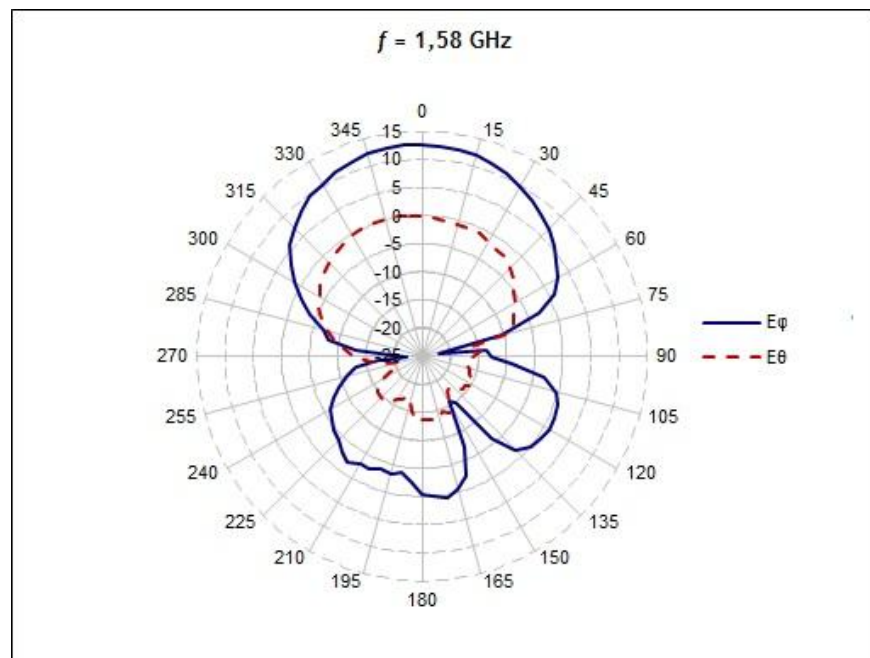


Figure 5.11 - Comparison between polar plots of E_ϕ and E_θ radiation patterns measured for $f_2 = 1.58$ GHz

Looking at the radiation pattern differences one can see that its unidirectionality is once again a feature, with some back lobes. The gain is high and is equal to 12.6 dB in the E_ϕ plane. On the other hand, HPBW is equal to 65 degrees at the same plane.

5.2.3 Measurement of f_3

The radiation pattern measured for $f_3 = 1.69$ GHz is plotted in Figure 5.12 as a polar plot of E_φ , and in Figure 5.13 as a polar plot of E_θ . The comparison between both patterns is made in Figure 5.14.

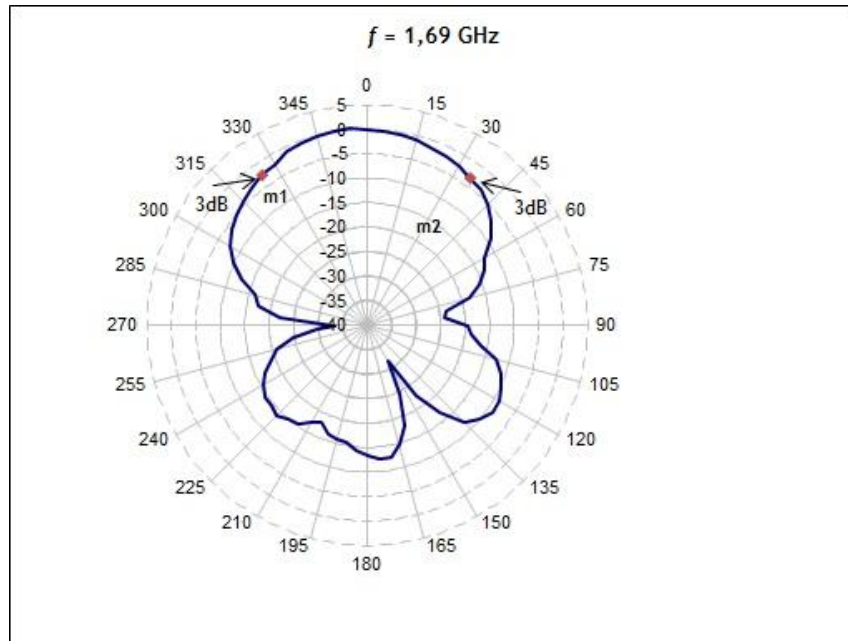


Figure 5.12 - Polar plot of the radiation pattern of E_φ measured for $f_3 = 1.69$ GHz

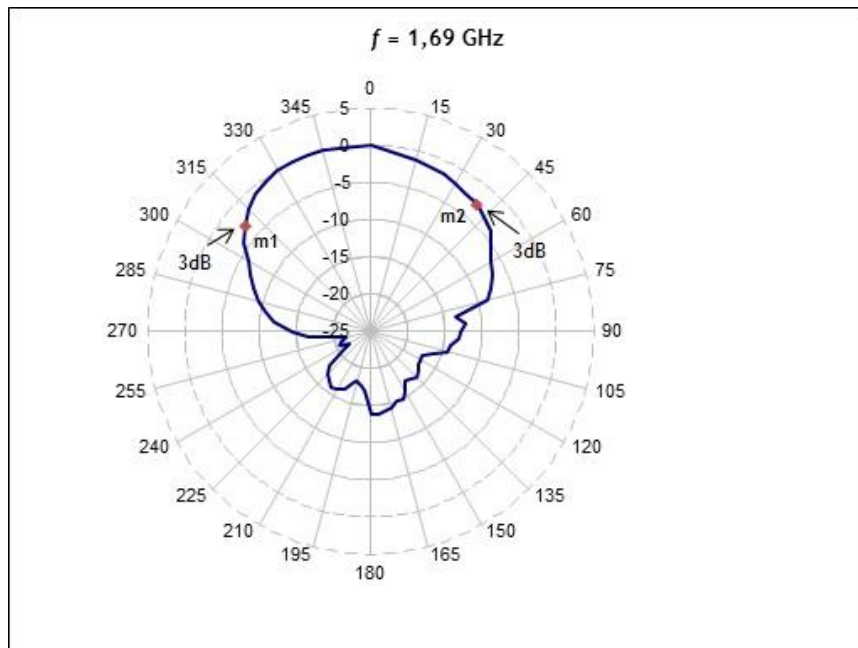


Figure 5.13 - Polar plot of the radiation pattern of E_θ measured for $f_3 = 1.69$ GHz

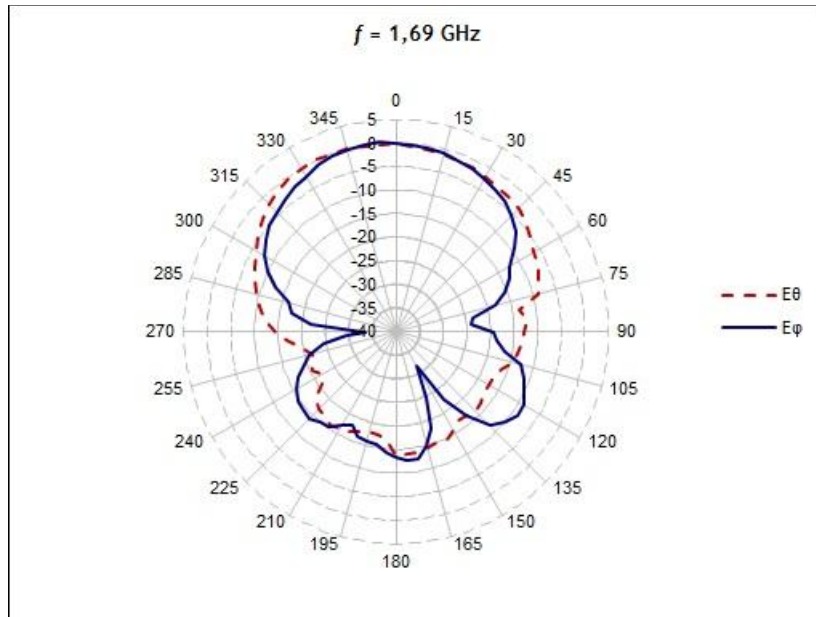


Figure 5.14 - Comparison between polar plots of E_ϕ and E_θ radiation patterns measured for $f_3 = 1.69$ GHz

Looking at the radiation pattern differences, its unidirectionality is still a feature, with some back lobes again; although, now the gain is only 0.3 dB at the E_ϕ . On the other hand, HPBW is equal to 70 degrees at the same plane.

5.2.4 Measurement of f_4

The radiation pattern measured for $f_4 = 2.384$ GHz is plotted in Figure 5.15 as a polar plot of E_ϕ , and in Figure 5.16 as a polar plot of E_θ . The comparison between both patterns is made in Figure 5.15.

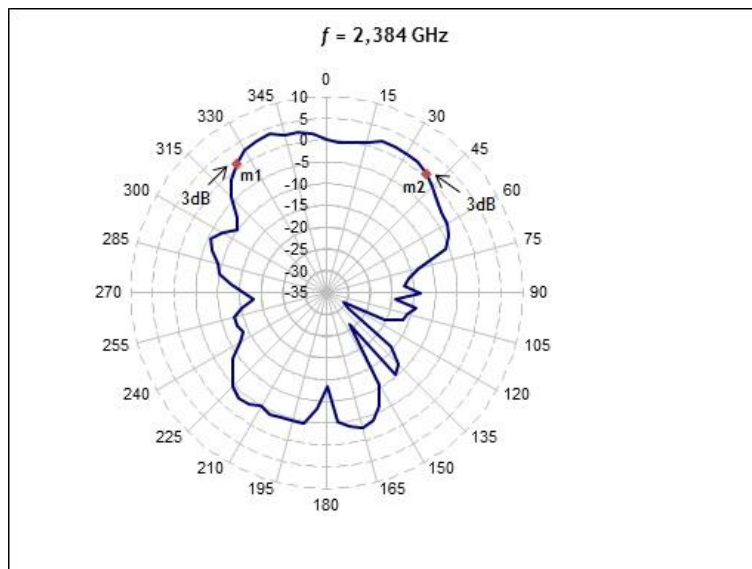


Figure 5.15 - Polar plot of the radiation pattern of E_ϕ measured for $f_4 = 2.384$ GHz

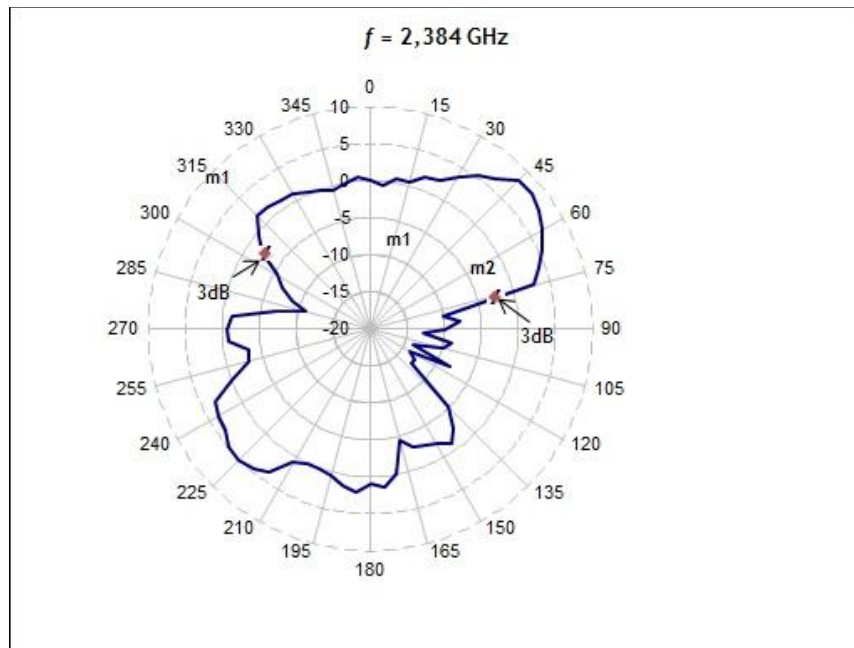


Figure 5.16 - Polar plot of the radiation pattern of E_θ measured for $f_4 = 2.384$ GHz

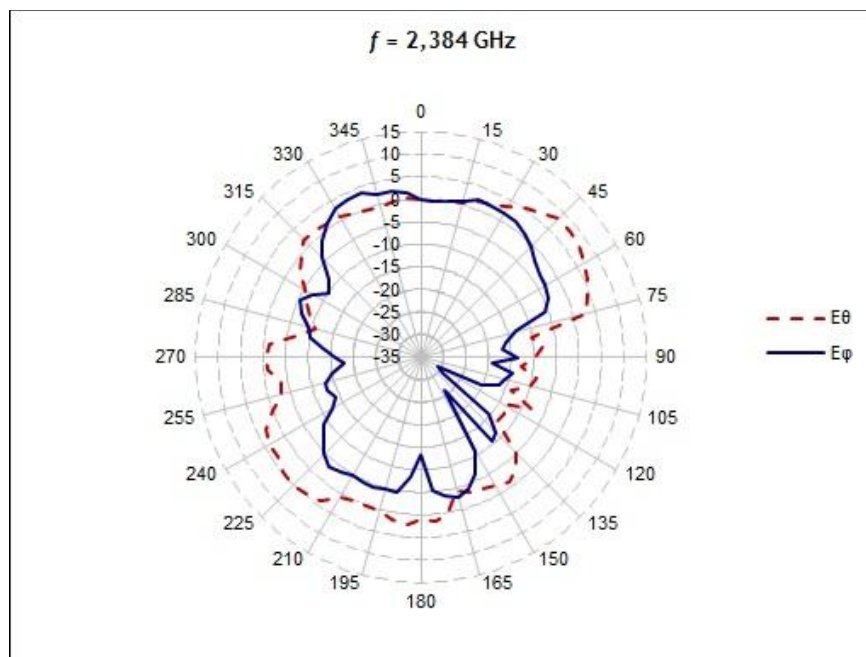


Figure 5.17 - Comparison between polar plots of E_ϕ and E_θ radiation patterns measured for $f_4 = 2.348$ GHz

Now, the radiation pattern starts to behave less unidirectional, although, some properties are still of unidirectionality are still seen. The back lobes are more. The gain is equal to 3.7 dB in the E_ϕ . On the other hand, HPBW is equal to 75 degrees at the same plane.

5.2.5 Measurement of f_5

The radiation pattern measured for $f_5 = 2.516$ GHz is plotted in Figure 5.18 as a polar plot of E_φ , and in Figure 5.19 as a polar plot of E_θ . The comparison between both patterns is made in Figure 5.20.

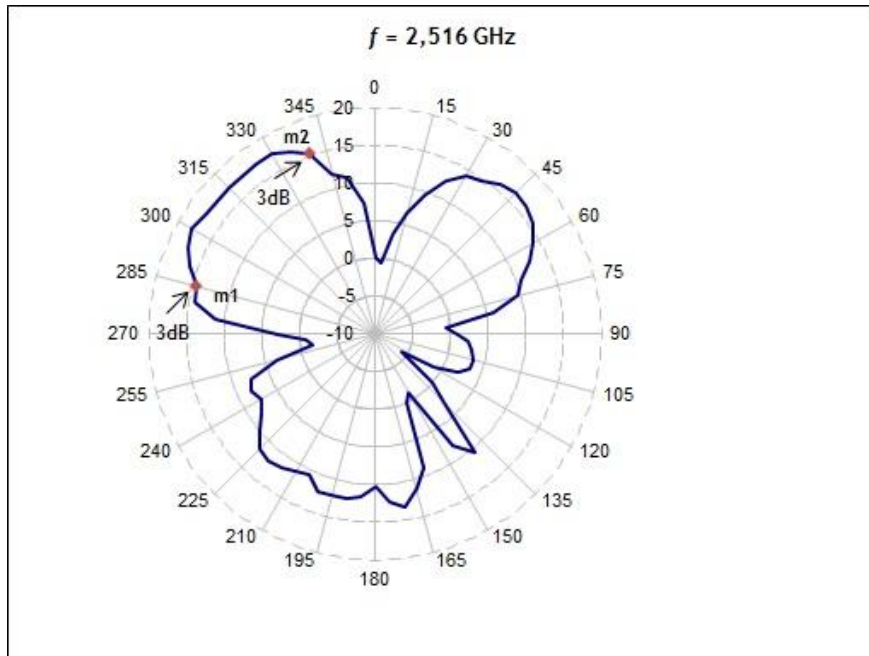


Figure 5.18 - Polar plot of the radiation pattern of E_φ measured for $f_5 = 2.516$ GHz

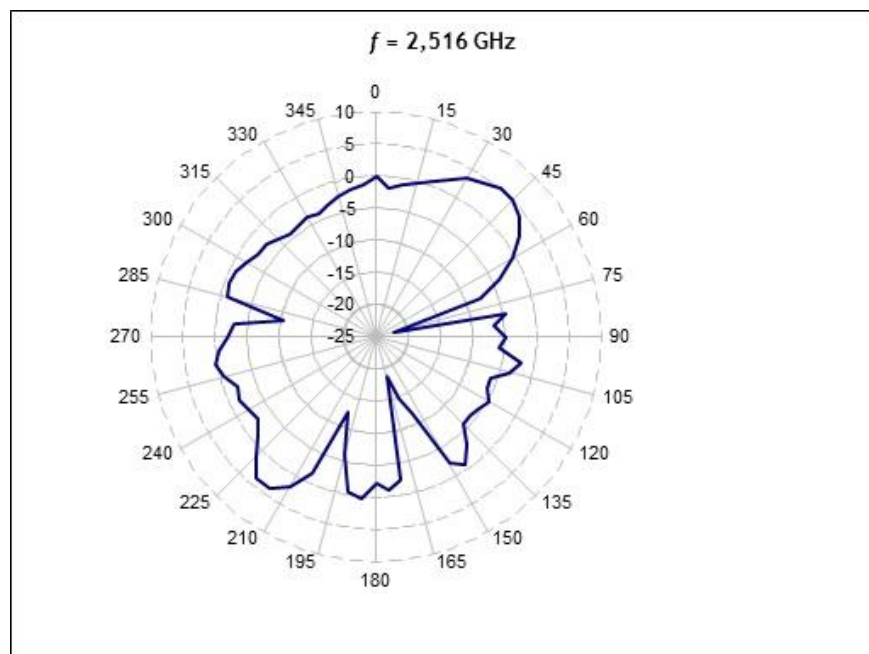


Figure 5.19 - Polar plot of the radiation pattern of E_θ measured for $f_5 = 2.516$ GHz

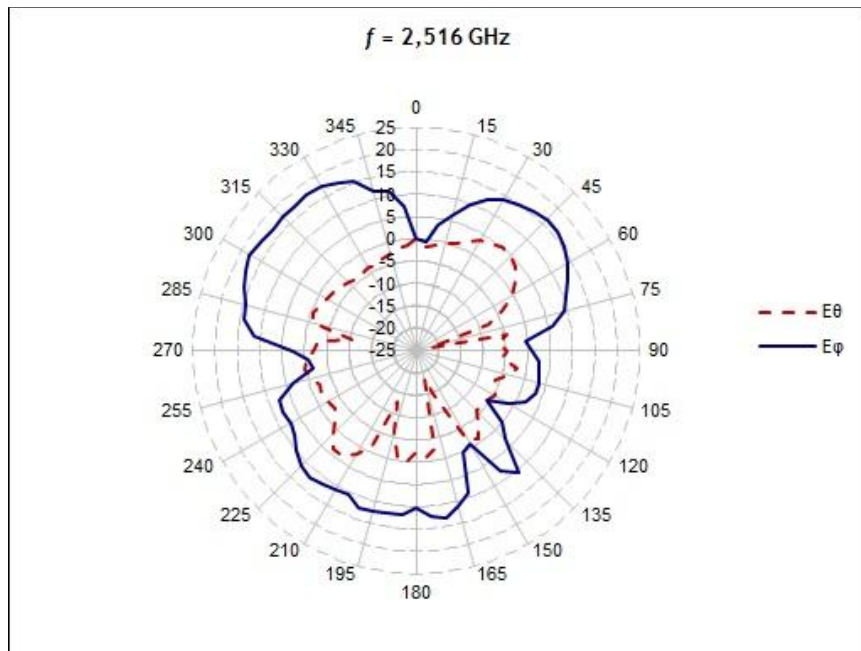


Figure 5.20 - Comparison between polar plots of E_ϕ and E_θ radiation patterns measured for $f_s = 2.516 \text{ GHz}$

Looking at the radiation pattern differences one can see that its unidirectionality is not properly a feature in this case. The gain is high and is equal to 12.6 dB in the E_ϕ . On the other hand, HPBW is equal to 55 degrees at the same plane. Unfortunately, E_ϕ has not a measurable directivity.

Finally, the HPBW is compared for each radiation pattern in Table 5.3.

Table 5.3 - HPBW for the several tested frequencies

Frequency (GHz)	Beamwidth $\alpha=0(\text{degrees})$	Beamwidth $\alpha=90(\text{degrees})$
1.274	70	70
1.58	65	95
1.69	70	90
2.384	75	Not available
2.516	55	Not Available

Chapter 6

Conclusions and Future Work

6.1 Analysis and review

The main objective of this thesis was to design a broadband feed working in a 3.75:1 bandwidth; that is, operating in a frequency range of 800 MHz to 3 GHz. At the beginning of the work, the feeding of the antenna was not working as wished; although, with the improvement of the method of feeding, PESA started to behave more like a broadband antenna. This can be observed knowing that return loss for the most of the frequencies is below -10dB, and the VSWR is the most of the times under the upper limit 2, which is a requirement for a good impedance matching. The radiation pattern was also working as wished at the most of tested frequencies, such as: 1.274 GHz; 1.58 GHz; 1.69 GHz; and 2.384 GHz. Only the last frequency tested (2,516 GHz) was not working as the others. In fact, that frequency has a slightly difference comparing to the simulated value.

Apart from that, the proposed tasks were successfully achieved, such as: the implementation of the planar equiangular spiral antenna; its characterisation and calibration of the feed in VNA; and its feeding with the coaxial cable.

About the difference between the simulated results and the measured results, the return loss seems to be concordant to the important bandwidth, where PESA radiates, apart from the differences in the peak values of the different frequencies. The relationship of VSWR with return loss is implicit; thus it follows the same reasoning.

About the radiation pattern measurements, the following tables establish the comparison of simulated results and measured results:

Table 6.1 - Measured vales of radiation pattern measurements

Frequency (GHz)	Beamwidth $\alpha=0(\text{degrees})$	Beamwidth $\alpha=90(\text{degrees})$	Gain in E_{φ} (dB)
1.274	70	70	1.74
1.58	65	95	12.6
1.69	70	90	0.3
2.384	75	Not available	3.7
2.516	55	Not Available	12.6

Table 6.2 - Simulated values of radiation pattern measurements

Frequency (GHz)	Beamwidth $\alpha=0(\text{degrees})$	Beamwidth $\alpha=90(\text{degrees})$	Gain in E_{φ} (dB)
1.274	84	73	10.221
1.58	103	92	5.8006
1.69	63	47	9.4707
2.384	61	80	20.6775
2.516	52	110	20.6775

As observed, there are slightly differences in the gain; although, the HPBW is very concordant for the most of the values.

Finally, it is important to state that despite of some aspects have been left behind due to the limited available time, the project in an overall was successfully achieved.

6.2 Future Work

In the nearby future, the need to improve the obtained results is a requisite. As analysed, PESA is already behaving as a good antenna, despite of some contretemps, though still some improvements are necessary. An improved impedance matching of the planar equiangular spiral antenna can be done, despite of being a complex matter. The problem about measuring the radiation pattern at the anechoic chamber in a more sophisticated way is also affecting the results taken. Therefore, the necessity of doing the measurements again is a future requisite to confirm the good results.

The lack of available time to test all the planned conditions was another factor; thus, the installation of the planar equiangular spiral antenna (shown in Figure 3.8), as a feed of the parabolic antenna of FEUP for the tracking of satellites, will be done as soon as possible. Even though the background of this thesis (see 2.8) refers to satellite systems and their connection is established with ground antennas, the practical tests still need to be done in order to achieve an excellent performance of all the requirements discussed before the beginning of this thesis.



Figure 6.1 - Parabolic antenna which will be part of a future work

References

- [1] C. A. Balanis, "Antennas," in *Antenna theory : analysis and design*, 2nd ed New York: Wiley, 1997, pp. 1 - 7.
- [2] J. D. Kraus, "Basic Antenna Concepts," in *Antennas*, 2nd ed New York: McGraw-Hill, 1988, pp. 17 - 19.
- [3] J. D. Kraus and R. J. Marhefka, "Antenna Basics," in *Antennas for all Applications*, 3rd ed New York: McGraw-Hill, 2002, pp. xviii, 938 p.
- [4] GEOG 3110 - *The Earth From Space: Remote Sensing of the Environment*. Available: <http://www.geog.utah.edu/~pdennison/geog3110.html>
- [5] *Definition of frequency bands* Available: <http://www.vlf.it/frequency/bands.html>
- [6] *Radar Terms and Definitions*. Available: http://www.interfacebus.com/Electronic_Dictionary_Radar_Terms_Lo.html
- [7] C. A. Balanis, "Fundamental Parameters of antennas," in *Antenna theory : analysis and design*, 2nd ed New York: Wiley, 1997.
- [8] A. Hollister. (2007, Scattering Parameters & Smith Charts *Smith Charts*
- [9] (October 2010). *Antennas*. Available: <http://www.antenna-theory.com>
- [10] J. L. Volakis, "Fundamentals of Antennas, Arrays, and Mobile Communications," in *Antenna engineering handbook*, 4th ed New York: McGraw-Hill, 2007, pp. 13 - 14.
- [11] P. Palmer. October 2010). Introduction to antennas. Available: http://courses.ee.sun.ac.za/HF_Technique_414/
- [12] W. L. Stutzman and G. A. Thiele, "Broadband Antennas," in *Antenna theory and design*, 2nd ed New York: J. Wiley, 1998, pp. 260 - 261.
- [13] C. A. Balanis, *Antenna theory : analysis and design*, 2nd ed. New York: Wiley, 1997.
- [14] *EEtasia*. Available: http://www.eetasia.com/ART_8800367192_480600_NP_3371d6b7.HTM
- [15] J. Thaysen, *et al.*, "A logarithmic spiral antenna for 0.4 to 3.8 GHz," *Applied Microwave & Wireless* vol. 13, p. 32, February 2001.
- [16] J. D. Dyson, "The equiangular spiral antenna," *IRE Transactions on Antennas and Propagation*, vol. AP-7 : IEEE, pp. 181-187, 1959.
- [17] R. Geurts, "Broadband Feeds for Integrated Lens Antennas," M.S. thesis, Division of Telecommunication Technology and Electromagnetics, Faculty of Electrical Engineering Eindhoven University of Technology Eindhoven, Netherlands, 2002.
- [18] J. D. Kraus, "Broadband and Frequency-Independent Antennas," in *Antennas*, 2nd ed New York: McGraw-Hill, 1988.
- [19] V. H. Rumsey, "Frequency Independent Antennas," *IRE National Convention Record*, vol. 5, pp. 114-118, 1957.
- [20] SAC. (December 2010). *Satellite Communications - An overview*. Available: <http://www.sac.gov.in/>
- [21] M. J. Leitão, *Sistemas de Comunicação por Satélite - Sistemas de Radiocomunicação*: Faculdade de Engenharia da Universidade do Porto.

- [22] (October 2010) *MATLAB*. Mathworks. Available: <http://www.mathworks.com/products/Matlab>
- [23] (October 2010). *Ansoft Electronic Design Products, Ansoft HFSS* Available: <http://www.ansoft.com/products/hf/hfss>
- [24] A. E. E.-A. Technologies. *ADS*. Available: <http://www.home.agilent.com/>

Appendix A

Matlab Code

```

%%%%%%%%%%%%%%%%%%%%%%%%%%%%%%%%%%%%%%%%%%%%%%%%%%%%%%%%%%%%%%%%%%%%%%%% Drawing of the Planar Equiangular Spiral Antenna %%%%%%%%%%%%%
close all
clear all

a = 0.35
K = 0.597 % Width along the defined radius
phi = [0:1/200:1+3/8]*2*pi; % The angle of rotation
arm = exp(a*phi);
lambda = 3e8*0.8/800e6 * 1000; % wavelength
factor = lambda / (0.5*(1+K)*(max(arm)-min(arm))*sqrt(1+1/a/a))

x_b1 = real(factor*arm.*exp(j*(phi+pi/4)));
y_b1 = imag(factor*arm.*exp(j*(phi+pi/4)));

x_b2 = real(factor*arm.*exp(j*(phi+pi/4))*K);
y_b2 = imag(factor*arm.*exp(j*(phi+pi/4))*K);

x_r1 = real(factor*arm.*exp(j*(phi+pi+pi/4)));
y_r1 = imag(factor*arm.*exp(j*(phi+pi+pi/4)));

x_r2 = real(factor*arm.*exp(j*(phi+pi+pi/4))*K);
y_r2 = imag(factor*arm.*exp(j*(phi+pi+pi/4))*K);

x_b = [x_b1(1);x_b2;flipud(x_b1)];
y_b = [y_b1(1);y_b2;flipud(y_b1)];

```

```

x_r = [x_r1(1);x_r2;flipud(x_r1)];
y_r = [y_r1(1);y_r2;flipud(y_r1)];

x_circ1 = real(factor*max(arm)*K*exp(j*(0:1/pi/20:2*pi)));
y_circ1 = imag(factor*max(arm)*K*exp(j*(0:1/pi/20:2*pi)));

x_circ = [ x_circ1 x_circ1(1)];
y_circ = [y_circ1 y_circ1(1)];

x_sqr = real([1-j 1+j -1+j -1-j 1-j]*0.5*200);
y_sqr = imag([1-j 1+j -1+j -1-j 1-j]*0.5*200);

hold off
plot(x_b,y_b);
hold on
plot(x_r,y_r,'r');

plot(x_circ,y_circ,'g')

plot(x_sqr,y_sqr,'m')
plot(factor*max(arm)*K*exp(j*(0:1/pi/20:2*pi)), 'g-')

zx = x_b;
val = y_b;

zx2 = x_r;
val2 = y_r;

zx3 = x_circ;
val3 = y_circ;

zx4 = x_sqr;
val4 = y_sqr;

axis equal
hold off

```

Appendix B

Calibration Types

A vector network analyser has several types of calibration. Usually, each calibration has its own properties and terms, so the user can obtain the required calibration. The general properties for deciding the type of calibration to use are the scattering parameters that are necessary to measure, and the errors which can be associated with them. Therefore, the necessity of following a plan to correct those errors comes up. Now, a set of terms are described in order to understand how calibrations are done.

- Calibration type: Specifies the type of necessary calibration to correct errors. In this thesis the type of calibrations used are the Full one-port calibration and the one-path two-port calibration.
- Standard procedure: A match, a short, an open, or a through standards can be used depending on the calibration type and on the errors to be corrected. Open and short standards are used to acquire the reflection tracking error and the source match, respectively; while the match standard is used to acquire the directivity error. The through standard is used to give the transmission tracking error.
- Scattering parameters to measure: S_{11} (measured at input port 1), S_{22} (measured at output port 2), or S_{12} parameters can be measured.
- Error before calibration: Specifies the type of errors which can be corrected by a specific standard procedure.
- Application after correction: Allows the measurement of wanted parameters (S_{11} , S_{22} , S_{12} , and VSWR) after the calibration corrections.
- Correction accuracy: Gives an idea of how precise are the calibration corrections.

Next, a table with the description of each calibration type is given (only the calibration types used in this thesis are referred).

Table B.1 - Calibration information

Calibration type	Standard procedure	Scattering parameters to measure	Errors before calibration	Application after correction	Correction accuracy
Full one-Port	Open; short; match	S_{11} or S_{22}	Reflection tracking error; directivity error	Reflection measurements of S_{11}	High
One-path two-port calibration	Open; short; match; through	S_{11} , S_{21} or S_{12}	Reflection tracking error; directivity error; transmission tracking error	Transmission in one way measurements	Medium to high